We thank both reviewers for their positive and constructive comments. We address their specific points below:

Reviewer 1: Bill Asher

*I think the authors are glossing over a potential problem in that in the system they are studying, CO_2 is an invasive flux (air-to-ocean) and DMS is an evasive flux (ocean-to-air). My hunch is that Equation 5 is only strictly true when both gases are far from equilibrium *and* the flux is in the same direction. Problems arise in applying Equation 5 for a mixed system, where one gas is invading and one is evading, because the bubble gas flux is not the same, even when normalized to a common diffusivity/solubility. In the case of invasion, the bubble overpressure drives more gas than expected (based on the bulk air-ocean concentration difference) into the water.*

This is true, and we are glad that you brought it up. However, it is a small effect. Woolf (1997) provides the means to calculate the magnitude of this effect. The average fractional extra pressure on the gas in contact with the sea (Δ) can be estimated from:

$\Delta = (U/U_i)^2\%$

where Ui is the wind speed at which the supersatuation of a particular gas equals 1% (49 m s^{-1} for CO_2). A high wind speed (20 m s^{-1}) gives $\Delta = 0.167\%$. An atmospheric pCO_2 of 400 ppm implies that the bubble overpressure would be 0.67 ppm. This is a ~2% enhancement of the CO_2 flux when the air/sea concentration gradient is small (minimum for this study = 30 ppm). Larger air/sea concentration gradients would diminish the magnitude of the bubble overpressure further.

We have added the following text to our revised manuscript after equation 5:

"Strictly speaking, Equation 5 should also account for the influence of bubble overpressure, which alters the gas flux due to bubbles when the concentration gradient is toward the ocean. The extra pressure on the gas in the bubbles is calculated following Woolf (1997): $\Delta = (U_{10}/U_i)^2$ % where U_i is the wind speed at which the supersaturation of a particular gas equals 1% (49 m s^{-1} in the case of CO_2). A high wind speed (20 m s^{-1}) gives $\Delta = 0.167\%$, which would lead to a

~2% enhancement of the CO_2 flux when the air/sea concentration gradient is 30 ppm (minimum for this study) and into the ocean. The magnitude of this effect would be larger for gases less soluble than CO_2 but we are able to ignore it for the purposes of this study."

one thing is clear from looking at the material in the supplements, is that using the Asher et al. (2002) relationship for both CO2 (invasion) and DMS (evasion) is not correct. The Asher et al. (2002) relation is only for invasion. For evasion, there is a separate equation in Asher and Wannninkhof (1998).

This is also true and we are glad that it has been pointed out. As the bubble term for DMS is small, there will be negligible impact upon our data. To be absolutely correct, we have adjusted our data and the relevant equations in the revised manuscript.

Line 54: "These processes include ..." Comment: Buoyancy effects are not a process. It might be better in this sentence to say something like "These processes include diffusion, surface renewal, and bubble-mediated transport. In turn, turbulence can be generated by wind stress, wave-induced mixing, buoyancy currents, and wave breaking."

Change made.

Line 56: "A variety of theoretical, laboratory, and field ..." Comment: I don't think this sentence is strictly true. My opinion is we have a fairly good understanding of the factors that affect gas exchange from a phenomenological standpoint (the authors list them just a couple of sentences earlier). What we lack is how to determine which of those processes are important under a given set of circumstances.

Changed sentence to:

"A variety of theoretical, laboratory, and field approaches have been used to study the processes that control air/sea transfer, but we do not yet have a firm understanding of their relative importance under a range of atmospheric and oceanic conditions."

Line 60: "Gas transfer via bubbles (k_bub) ..." Comment: It would be good to define k_bub here. The point is that there are a couple of different ways to do this, you can go the Memery and Merlivat (Memery, L. and L. Merlivat (1985). "Modeling of the gas flux through bubbles at the air-water interface." Tellus, Ser. B 37: 272-285) approach and use the bulk air-water concentration difference and accept that k_bub for invasion and evasion are different (e.g., I used this approach in Asher et al. (1996, JGR-Oceans)) or you can redefine the air-water concentration difference in terms of how bubbles would affect the equilibrium and have a common k_bub (but then it might get complicated relating k_bub for invasion and evasion) as done by Woolf (1997).

We have clarified the definition of k_bub here and cover the issue of invasion vs evasion in detail on Line 161 (to address the comment below).

Line 78: "These measurements typically show DMS gas transfer velocities that are lower and exhibit more linear wind speed dependence than those estimated for CO2 based on dual tracer studies (e.g. Bell et al., 2015; Yang et al., 2011; Goddijn-Murphy et al., 2012)." Comment: I think the authors should be clear here that there are no CO2 measurements from dual-tracer studies. There are DT measurements for SF6/He, which get related to CO2 through diffusivity. Then there are EC measurements for CO2. Comparison of the DT-derived CO2 transfer velocities with CO2 transfer velocities produced by EC measurements of CO2 fluxes shows relatively good agreement. It is the transfer velocities produced by EC measurements of DMS fluxes that show different behavior.

Change made.

Line 87: Comment: maybe want to note that they agree when normalized to a common diffusivity.

Change made.

Line 126: "The air side gas transfer contributes about 5% on average to the total resistance for DMS." Comment: The air-side resistance fraction is a function of wind speed. Does this

5% increase as U increases? COAREG must reproduce this, it was measured by McGillis et al. a while back.

McGillis et al.. (2000) used a non-linear relationship between waterside transfer velocity and wind speed. Based on more recent measurements of DMS gas transfer velocity it is more appropriate to assume a linear relationship. As a result, the relative contribution of airside resistance to total resistance does not change substantially as a function of wind speed (see Supplemental material in Bell et al 2015).

Line 161: the relation in the text showing k_w = k_int + k_bub. Comment: I wonder if maybe it is time to stop writing this as a general expression (I know, I am guilty of this as well). What is generally true is that the total gas flux is equal to the sum of interfacial flux and the bubble flux. Saying the overall transfer velocity is equal to the sum of the two transfer velocities really only works if the concentration difference is far from equilibrium. Work through David's relations from the 1997 paper and you'll find they are a bit convoluted in terms of how exactly the pieced (his Delta term) fit together to make a coherent physical picture. If you start by assuming it is the fluxes, not the transfer velocities, which sum linearly, the assumptions required to get to the various relations proposed are more easily understood.

We have changed the text to be more accurate.

Technical Comments:

1. Multiple citations are not in any recognizable order. Sometimes they are chronological, sometimes alphabetical. I don't remember what the ACP style guide says, but I am sure it is not "random."

Agreed! We will correct this.

2. Line 74: "... studies indicate a non-linear dependence ..."

Changed to "studies observed a non-linear wind speed dependence"

Line 91: Shouldn't cite papers that are not published or submitted.

OK, removed.

Line 175: The two f values are opposite from what is given in the supplement. Not sure which is correct, but it should be consistent (and correct).

Good spot. Changed in the supplemental material.

Line 323: I know this is petty, but I don't think Woolf (1997) is based on laboratory data.

Woolf (1997) did use laboratory data from other studies. We will clarify this.

Equation 7: Figure caption says "cubic" and equation 7 is quadratic. Resolve this difference.

Changed.

Line 384: The citation to Asher and Wanninkhof (1998) should be to Asher et al. (1996). If you really must cite Asher and Wanninkhof (1998) in this context, which you shouldn't, at least make it the other Asher and Wanninkhof (1998) paper that is directly relevant (see citation above).

Changed.

Reviewer 2: Ian Brooks

Line 86-87: "In that study, no statistically significant difference was observed in gas transfer-wind speed relationships of CO2 and DMS for winds below 10 m s-1" – need to clarify this statement, was a significant difference found for winds above 10 m s-1? Was 10 m s-1 the maximum wind speed in the study?

Changed to:

"In that study, no data were collected for winds greater than 10 m s-1 and no statistically significant difference was observed in the CO2 and DMS gas transfer-wind speed relationships."

Line 104-105: as noted in the comment from Blomquist, the air-side resistance is not a function of solubility (though its contribution to the derivation of waterside transfer velocity is dependent on solubility).

This has been corrected.

Line 122-123: The use of the COAREG 3.1 model to calculate air-side transfer velocities in order to derive the waterside transfer velocity introduces an assumption that COAREG is providing valid values of ka. Any uncertainty in this will impact the later results and should be acknowledged and if possible quantified.

We have added the following sentence:

"Note that the use of the COAREG 3.1 model introduces a small uncertainty in our estimates of waterside DMS gas transfer velocity (approximately ±2% when wind speed = 20 m s^{-1})."

Line 126-127: "The air side gas transfer contributes about 5% on average to the total resistance for DMS" – do you mean 'air-side resistance' rather than air-side transfer?

Yes. Changed.

Line 140: "...(Equation 4)..." should be "...(Equation 3)..."

Line 170: "...into Equation 6 yields..." should be "...into Equation 5 yields..."

Changed.

Line 192 - figures: Figures 1 and 2 are introduced here, but figure 2 is not actually discussed until after discussion of figure 4 breaking the flow of discussion and figures, and leaving me, initially, confused as to how I'd missed the discussion of figure 2. In fact, only the general

environmental conditions shown in figure 1 are discussed here, not the gas flux results, which are discussed much later. Figure 1 would be better split into 2, separating the gas fluxes into a figure matching the format of current figure 2. The figures showing the gas flux results could then be placed in a logical order within the discussion. Since wave state is a relevant parameter in the later discussion, it would be useful to add a time series of at least significant wave height to figure 1.

We agree. Figure 1 has been split and a timeseries of Hs has been added. Figures are reordered so the gas flux/transfer velocity figures follow the whitecapping figures.

Line 207: The authors note that their estimates of whitecap fraction as a function of wind speed are substantially lower than other recently published values – at times an order of magnitude lower. A likely reason for this is the exposure settings on the camera. During the HiWinGS project cruise in 2013 two independent sets of cameras were used for whitecap imaging. They were initially found to give whitecap fractions that differed by a factor of several. Tests were conducted during the final transit of the cruise, in which a pair of identical cameras were run side by side; one with fixed exposure settings, the other having the exposure settings changed every few hours. The exposure settings were found to make a substantial difference to the whitecap fraction calculated using the same Callaghan and White (2009) algorithm used here – up to a factor of 4 for the range of settings tested. It was found that almost all of this difference (both between the 2 cameras in the exposure trial, and between the two sets of cameras used throughout the cruise) was removed if the images were first 'normalised' to remove any brightness gradient across the image. Brief details of these tests will be given in

Brumer, S. E., C. J. Zappa, I. M. Brooks, H. Tamura, S. M. Brown, B. Blomquist, C. W. Fairall, A. Cifuentes-Lorenzen, 2017: Whitecap coverage dependence on wind and wave statistics as observed during SO GasEx and HiWinGS, J. Phys. Oceanogr. (under revision)

Many of the potential issues highlighted above (exposure settings, intercomparability of image processing) have actually been addressed. We have added additional information about the whitecap image processing to the Supplemental material.

The lower bounds of the Knorr *W* data do fall below recent parameterisations, most notably in the wind speed range of ~ 7.5 m s^{-1} to 12.5 m s^{-1}. However, when the Knorr *W* data are binned

by wind speed (squares in Figure 3a, main manuscript), the binned *W* data compare favourably with the Schwendeman and Thomson (2015) estimate of whitecap fraction at all wind speeds, with the exception of the lowest bin of 3 m s^{-1}. The binned Knorr *W* data also agree favourably with Callaghan et al., (2008), except for the 9 m s^{-1} and 11 m s^{-1} binned datapoints, for which the Knorr binned *W* data are lower. When binned by wind speed, the Knorr *W* data and the two parameterisations generally fall within a factor of 2 across the wind speeds examined.

There is clearly quite a lot of scatter in the Knorr *W* dataset, and many data points lie below the Schwendeman and Thomson (2015) and Callaghan et al., (2008) parameterisations. However, we do not believe that the primary driver of the differences observed is due to the image processing methodology employed. Rather, it could be that other sources of variability (at a given wind speed) have caused the observed differences. Examples include: (i) water chemistry (surfactants); (ii) total wave field energy dissipation; and (iii) energy dissipation by microscale breaking waves as opposed to air-entraining whitecaps. It is beyond the scope of this paper to address these potential causes.

Line 213-215: "Stage A whitecap fraction data is highly variable at ~11 m s-1 213 wind speeds (Figure 3b), which is driven by the difference in the wind-wave conditions during Knorr_11 (ST184 vs ST191, Figure 4a)" – two points:

(1) the difference is ascribed to different wind-wave conditions at the two stations, but no wave data are shown. As noted above, relevant wave parameters need to be added to figure 1.

Done.

(2) A similar broad range of stage A whitecaps is evident at around U = 6 m s-1, also resulting from grouping of high/low values by different stations...are the wind-wave conditions similarly different in this case?

We agree that there is a grouping at U=6 m s^{-1}. It is unclear what caused this (although ST181 was in the Gulf Stream and thus had much higher water temperatures). However, this discussion is beyond the scope of this paper.

Lines 218-223: The authors first note that where stage A whitecap fractions is < 10-4 the relationship with RH is more scattered than at higher fractions; they then note a number of factors that affect wave breaking and so whitecap fraction, but don't make a coherent link back to their initial point about the scatter in the stage-A whitecap / RH relationship. This reads as an almost unconnected series of statements...all true, but leaving the reader wondering what the point being made is.

We agree that this text needed adjusting. We also decided that the text discussing Stage A whitecap variability and R_H was not essential to the manuscript and have moved the modified text and the related Figure to Supplemental information.

Line 282: "...(Figure 5)" -> "...(Figure 5b,d)" – again text refers to high wave conditions for ST191 but no wave data provided for reader to assess.

In this instance, we feel that it is sufficient for us to reference the in depth discussion in Bell et al. (2013).

Figure 5 and the discussion of it have some general issues:

- It's hard to see the pink/green lines against the mass of pink/green dots on panels a and b – it

would help here to plot the dots in a paler shade of pink/green to allow the lines to stand out.

The figure has been adjusted to improve readability.

- The curves shown, for the COAREG3.1 model are a useful reference, but fits to the actual data

are also needed; these would allow a much clearer assessment of how closely the COARE model

agrees with the observations.

We tried this but it made the plots too busy. We decided it best not to include both.

- lines 282-284: "Under the high wind, high wave conditions encountered during ST191, the wind speed-dependence of kDMS,Sc was lower than expected, with a slope roughly half that of the rest of the cruise data. This effect was not observed at ST184." – since the ST191 data are not highlighted in any way it is not possible for the reader to judge the behaviour here. Of note perhaps is not simply the high wind and wave conditions during ST191 but the different time history of the winds – a sustained period of high winds during ST191 vs a very short period in ST184 where the wind rises rapidly, spikes, and decreases rapidly. These two periods are likely to produce very different wave fields at the same wind speeds – again, reason to plot the wave parameters in figure 1 – which might explain the very different whitecap fractions seen in Figure 1b for these periods.

In addition to plotting the wave data, we have added the word 'sustained' to this sentence and referenced Bell et al. 2013)

Line 294 & 305: the phrasing "until 11 m s-1 wind speed" is rather clumsy; 'until' implies a variation over time, which is not what is meant – "...up to wind speeds of 11 m s-1" would read better.

Change made.

Line 326: "...Δkw is near zero at very low wind speeds (U10 ≤ 4.5 m s-1)..." – this is hard to judge. Eyeballing the data points I would agree; however, there are only 3 points at U < 4.5 m s-1, and all of those at U>3 m s-1. Their mean Δk is ~5 cm/hr and the fitted curve approaches a Δkw of ~3 cm/hr at U = 0, not zero. One might argue for an alternative functional form in which the exponents were not prescribed might better represent the data; the quadratic used here implicitly assumes the functional dependence.

We have tested a variety of functional forms and number of exponents for our best fit: linear, polynomial (n=2,3), power (n=1,2) and exponential (n=1,2). The goodness of fit was extremely comparable between all fits (from $R^2 = 0.66$ to $R^2 = 0.67$) with the exception of the linear fit ($R^2 = 0.62$). As the goodness of fit did not help with our decision, the choice of fit is subjective. Having considered the different fit lines, we feel that a simple power law fit (Δk_w =

$0.177U_{10}^{1.928}$) represents the low Δk_w data better than our original choice of fit. We have changed the manuscript accordingly.

The fit line to the data tells us that Δk_w is indeed positive at low wind speeds. This could be driven by effects such as chemical enhancement and sea surface skin temperature (see Discussion), which we have not controlled for here. We used the term 'near zero' intentionally but now clarify this in the revised manuscript with "(< 4.5 cm/hr)"

What is the reasoning behind using 4-hour averages of transfer velocities here (and elsewhere)? 4

hours is quite a long time relative to the time period over which significant changes in forcing can take place. Granted it greatly reduces scatter, but I would wary of averaging over periods much long than ~1 hour.

Some averaging of the data was necessary to reduce the scatter, but we accept that minimising the averaging time period is important. We have changed our averaging period to two hours.

Line 358: "...the relationship between Δkw and whitecap areal extent appears to be linear." – I'm not convinced this is entirely true – approximately so over the range 0.005 < W < 0.05, but ~half the data points lie at W < 0.005, and seem to drop off rather more rapidly than the fit to the high values of W would indicate. Plotting W on a log scale might give a rather different impression. Not that IF the relationship is linear as suggested then eyeballing a fit (if you claim a linear fit, it would help to show it!) suggests Δk = 10-15 cm/hr at W = 0, which raises questions as to why that should be when there are no bubbles to account for a difference in k, and why this minimum difference is several times higher than that derived as a function of wind speed. If on the other hand a roughly linear fit of Δk to log(W) existed (which I think the rapid drop off in Δk at very low W might support) then Δk would approach zero at low W.

We have revised the statement to:

"The functional form of the relationship between Δk_w and whitecap areal extent appears to be linear for $W_T > 0.005$. However, the Knorr_11 dataset is small and quite scattered, particularly when $W_T < 0.005$."

316

317 *Line 366-367: "In this case, Δkw should be more strongly correlated with WA than WB or*
318 *WT." – in a general sense, this is true, but is only if the various factors affecting foam decay*
319 *vary. If foam decay rate is constant then WT should be proportional to WA.*

320 We agree. We feel this case is broadly covered later in the paragraph. We have adjusted the
321 text slightly to take into account a constant decay rate:

322 "W_T and W_A may be equally good (or poor) proxies for bubbles because: (i) surfactant activity
323 was either insignificant or sufficiently invariant in the study region (despite high biological
324 productivity) that W_B does not confound the relationship between W_T and W_A"

325

326 *Line 387: "Both models significantly underestimate kbub,CO2 at wind speeds below about 11*
327 *m s-1." Actually both models rather underestimate the observationally derived Kbub,CO2 at*
328 *all windspeeds; however, note that both models are driven by the observed wind-whitecap*
329 *relationship, which has already been stated to be low compared to other recent estimates. Is*
330 *the agreement better using a whitecap function that agrees more closely with the recent*
331 *consensus?*

332 The agreement is slightly improved (at intermediate wind speeds) using a different whitecap
333 function. Although we see no reason to doubt our whitecap measurements, it is useful to
334 observe the importance of the wind speed-whitecap fraction relationship to the output from
335 these models, so we have added these $k_{bub,CO2}$ estimates to the manuscript.

336

337 *While the Asher et al. model is lower than the observations, it is not wildly so (essentially*
338 *matching the lower boundary of the observed values), and the agreement in both values and*
339 *functional behaviour is rather convincing.*

340 We are possibly less optimistic on this point and hopefully can agree to disagree!

341

342 *Line 455: "...eddy covariance setup..." -> "...eddy covariance system..."*

343 Change made.

344

Line 463: reference to paper in preparation not generally allowed...if it's not 'in press' by the time this manuscript it copy edited, the copy editor will want the reference cut.

Change made.

Figure 3: it's hard to pick out the curves and black square points against the mass of black dots.

Suggest changing black dots to mid-grey and ensuring everything else is plotted over them. It would also be good to see a functional fit to this data as well as the functions from previous studies...especially as this function is later used to drive the kbub,co2 models plotted in figure 8.

Revised accordingly.

Estimation of bubbled-mediated air/sea gas exchange from concurrent DMS and CO_2 transfer velocities at intermediate-high wind speeds

Thomas G. Bell[1*], Sebastian Landwehr[2], Scott D. Miller[3], Warren J. de Bruyn[4], Adrian H. Callaghan[5,6], Brian Scanlon[2], Brian Ward[2], Mingxi Yang[1] and Eric S. Saltzman[7]

[1] Plymouth Marine Laboratory, Prospect Place, The Hoe, Plymouth, PL1 3DH, UK

[2] School of Physics, National University of Ireland, Galway, Ireland

[3] Atmospheric Sciences Research Center, State University of New York at Albany, NY, USA

[4] Schmid College of Science and Technology, Chapman University, Orange, California, CA, USA

[5] Scripps Institution of Oceanography, University of California San Diego, 9500 Gilman Drive, La Jolla, CA 92093

[6] Now at: Department of Civil and Environmental Engineering, Imperial College London, South Kensington Campus, London, SW7 2AZ, UK

[7] Department of Earth System Science, University of California, Irvine, CA, USA

*Correspondence to: T.G. Bell (tbe@pml.ac.uk)

Abstract

Simultaneous air/sea fluxes and concentration differences of dimethylsulfide (DMS) and carbon dioxide (CO_2) were measured during a summertime North Atlantic cruise in 2011. This dataset reveals significant differences between the gas transfer velocities of these two gases (Δk_w) over a range of wind speeds up to 21 m s^{-1}. These differences occur at and above the approximate wind speed threshold when waves begin breaking. Whitecap fraction (a proxy for bubbles) was also measured and has a positive relationship with Δk_w, consistent with enhanced bubble-mediated transfer of the less soluble CO_2 relative to that of the more soluble DMS. However, the correlation of Δk_w with whitecap fraction is no stronger than with wind speed. Models used to estimate bubble-mediated transfer from *in situ* whitecap fraction under-predict the observations, particularly at intermediate wind speeds. Examining the differences between

gas transfer velocities of gases with different solubilities is a useful way to detect the impact of bubble-mediated exchange. More simultaneous gas transfer measurements of different solubility gases across a wide range of oceanic conditions are needed to understand the factors controlling the magnitude and scaling of bubble-mediated gas exchange.

1 Introduction

Air/sea exchange is a significant process for many compounds that have biogeochemical and climatic importance. Approximately 25% of the carbon dioxide (CO_2) released into the atmosphere by anthropogenic activities has been taken up by the world oceans, which has tempered its climate forcing while leading to ocean acidification (Le Quéré et al., 2015). The biogenic gas dimethylsulfide (DMS) is a major contributor to the mass of marine atmospheric aerosol (Virkkula et al., 2006). Volatile organic compounds (VOCs) such as isoprene, acetone and acetaldehyde alter the oxidising capacity of the troposphere (Carpenter et al., 2012). The solubility differences between these VOCs mean that their exchange is controlled to differing degrees by processes on the water and air side of the air/sea interface (Yang et al., 2014). Many of the factors influencing air/sea gas exchange will be altered by future changes in climate, ocean circulation and biology. Earth system models and air quality models require more accurate understanding of the processes that influence air/sea gas transfer.

Air/sea gas exchange is typically parameterised as a function of the ocean/atmosphere bulk concentration difference (ΔC) and the physical mixing induced by wind stress at the interface (Liss and Slater, 1974). The air/sea flux is typically described using the expression:

$$Flux = K(C_w - \alpha C_a) \qquad \textit{Equation 1}$$

where C_w and C_a are the trace gas bulk concentration on either side of the interface, α is the dimensionless water/air solubility of the gas in seawater and K is the gas transfer velocity. The physics of gas transfer are implicitly represented by the gas transfer velocity, which is commonly expressed in water-side units of velocity (cm hr^{-1}) and parameterized as a function of wind speed (U_{10}) and Schmidt number (Sc). The simplicity of Equation 1 belies the complexity of the processes involved in air/sea gas transfer. These processes include diffusion, surface renewal~~, buoyancy effects, wave-induced mixing, wave breaking~~ and bubble-mediated transport. In turn, turbulence can be generated by wind stress, wave-induced mixing, buoyancy, currents and wave breaking. A variety of theoretical, laboratory, and field

approaches have been used to study these processes that control air/sea transfer, but we do not yet have a firm understanding of their relative importance ~~factors that control air/sea transfer~~ under a range of atmospheric and oceanic conditions.

The gas transfer-wind speed relationships for gases of different solubility may be affected by breaking waves and bubbles (Keeling, 1993; Woolf, 1993, 1997). Gas ~~transfer~~ invasion and evasion via bubbles (k_{bub}) is sensitive to the void fraction (ratio of air volume to total volume) of the bubble plume as well as the bubble size distribution. Bubble injection depth and cleanliness of the surface (influenced by surfactants) affect bubble rise velocity and residence time. Bubble residence time determines the time available for equilibration to occur while bubble volume, pressure and gas diffusivity (Sc) govern the time needed for a bubble to equilibrate. The magnitude of k_{bub} is expected to be greater for sparingly soluble gases (e.g. CO_2, dimensionless solubility ~1) than for more soluble gases such as DMS (dimensionless solubility ~15), particularly when bubbles are fully equilibrated. Bubble-mediated gas transfer has been studied in the laboratory (Asher et al., 1996; Rhee et al., 2007) and using models (e.g. Woolf, 2005; Woolf et al., 2007; Fairall et al., 2011; Goddijn-Murphy et al., 2016).

Deliberate, dual-tracer techniques have estimated gas transfer by measuring the evasion of a pair of sparingly soluble gases with different diffusivity (^{3}He and SF_6, dimensionless solubility ≤0.01). These studies ~~indicate~~ observed a non-linear wind speed dependence of the gas transfer velocity, in qualitative agreement with earlier studies in wind-wave tanks (e.g. Wanninkhof et al., 1985; Liss and Merlivat, 1986; Watson et al., 1991). Direct, shipboard measurements of waterside gas transfer have also been made by eddy covariance (e.g. McGillis et al., 2001; Huebert et al., 2004; Marandino et al., 2007; Miller et al., 2010; Bell et al., 2013). These measurements typically show DMS gas transfer velocities that are lower and exhibit more linear wind speed dependence than ~~those~~ the CO_2 transfer velocity-wind speed relationship inferred from~~estimated for CO_2 based on~~ dual tracer studies (e.g. Yang et al., 2011; Goddijn-Murphy et al., 2012; Bell et al., 2015). It has been suggested that the difference between the open ocean gas transfer velocities of CO_2 and DMS is due to the reduced importance of bubble-mediated exchange for DMS (Blomquist et al., 2006; Fairall et al., 2011; Goddijn-Murphy et al., 2016).

Only one set of concurrent CO_2 and DMS gas transfer velocity measurements have been published to date (Miller et al., 2009). In that study, no data were collected for winds greater

than 10 m s^{-1} and no statistically significant difference was observed in the CO_2 and DMS gas transfer-wind speed relationships after normalising both gases to a common diffusivity. ~~In that study, no statistically significant difference was observed in gas transfer-wind speed relationships of CO_2 and DMS for winds below 10 m s^{-1}.~~ This study presents a more extensive set of CO_2 and DMS gas transfer velocities that were measured simultaneously aboard the R/V Knorr in the 2011 summertime North Atlantic in both oligotrophic and highly productive waters. The DMS ~~and CO_2~~ gas transfer velocities are discussed separately in detail by Bell et al. (2013) ~~and Miller et al., In Prep~~. Here we focus specifically on what can be learned about gas transfer from the differences in behaviour of two different solubility gases at intermediate and high wind speeds.

2 Methods

2.1 Seawater, atmospheric and flux measurement systems

The measurement setups for DMS and CO_2 concentrations in air and water and the eddy covariance flux systems have been discussed in detail elsewhere (Miller et al., 2008; Saltzman et al., 2009; Miller et al., 2010; Bell et al., 2013; Landwehr et al., 2014; Bell et al., 2015; Landwehr et al., 2015). We provide a summary plus~~and~~ some additional details in the Appendix ~~(Section 6)~~.

2.2 Gas transfer velocity calculations

In this section we describe the calculation of DMS and CO_2 gas transfer velocities from the Knorr_11 cruise data. Measured gas transfer velocities are transformed into water side only gas transfer velocities in order to remove the influence of air-side resistance. The relative contribution of air-side resistance to the total resistance is a function of solubility and thus different for the two gases. Finally, we discuss the most appropriate approach for comparing the water-side gas transfer velocities, given that the two gases have different molecular diffusivity and solubility.

Total gas transfer velocities (K) are calculated for CO_2 and DMS for each 10-minute flux interval of the Knorr_11 cruise using Equation 1. The temperature-dependent dimensionless solubilities~~y~~ of CO_2 and DMS in seawater ~~is~~are calculated following Weiss (1974) and Dacey et al. (1984) respectively. These gas transfer velocities reflect the result of resistance on both

sides of the interface (Liss and Slater, 1974). The water side contribution to the total resistance is determined as follows:

$$k_w = \left[\frac{1}{K} - \frac{\alpha}{k_a}\right]^{-1} \qquad \textit{Equation 2}$$

where k_w and k_a are the air side and water side gas transfer velocities and α is dimensionless water/air solubility. Note that we use the α reported by Dacey et al. (1984) in these calculations rather than H as there appears to be an error in conversion between α and H in that study (see Supplemental information for discussion). CO_2 solubility is sufficiently low that air side resistance is negligible and the water side gas transfer is assumed equal to the total transfer velocity ($k_{CO_2} = K_{CO_2}$). The air side resistance for DMS needs to be accounted for because it is a moderately soluble gas (McGillis et al., 2000). Air side gas transfer velocities (k_a) for DMS were calculated for each 10 minute flux interval with the NOAA COAREG 3.1 model, using sea surface temperature (SST) and horizontal wind speed measured during the cruise. The NOAA COAREG 3.1 model (Fairall et al., 2011) is an extension of the COARE bulk parameterization for air/sea energy and momentum fluxes to simulate gas transfer (Fairall et al., 1998; Fairall et al., 2000). The air side ~~gas transfer~~resistance contributes about 5% on average to the total resistance for DMS. NOAA COAREG 3.1 model calculations were carried out using a turbulent/molecular coefficient, A = 1.6, and bubble-mediated coefficient, B = 1.8 (Fairall et al., 2011). Knorr_11 measurements of SST, air temperature, relative humidity, air pressure, downward radiation and wind speed were used as input parameters to the model. Note that the use of the COAREG 3.1 model introduces a small uncertainty in our estimates of waterside DMS gas transfer velocity (approximately ±2% when wind speed = 20 m s^{-1}).

To facilitate comparison of transfer coefficients for the two gases across a range of sea surface temperatures, gas transfer velocities are corrected for changes in molecular diffusivity and viscosity. The correction typically involves the normalisation of water side gas transfer velocities to a common Schmidt number (Sc=660), equivalent to CO_2 in seawater at 20°C:

$$k_{X,660} = k_X \cdot \left(\frac{660}{Sc_X}\right)^{-0.5} \qquad \textit{Equation 3}$$

where subscript x refers to CO_2 or DMS (i.e. $k_{DMS,660}$ and $k_{CO_2,660}$). Temperature-dependent Sc_{CO2} and Sc_{DMS} were obtained using the *in situ* seawater temperature from the ship's bow sensor and parameterisations from Wanninkhof (1992) and Saltzman et al. (1993).

The *Sc* number normalization (Equation 3~~4~~) is commonly used across the whole range of wind speeds. In fact, it is only appropriate ~~only for~~at low or moderate winds ~~in which~~when interfacial gas transfer dominates over bubble-mediated gas exchange. If bubbles are an important component of gas transfer then solubility also plays a role and normalization based on *Sc* alone may not be sufficient.

To develop a more rigorous comparison of k_{DMS} and k_{CO_2}, we normalized the water side transfer velocities of DMS to the Schmidt number of CO_2 at the *in situ* sea surface temperature of each 10-minute flux interval, as follows:

$$k_{DMS,Sc} = k_{DMS} \cdot \left(\frac{Sc_{CO_2}}{Sc_{DMS}} \right)^{-0.5} \qquad \textit{Equation 4}$$

where Sc_{CO_2} and Sc_{DMS} are the Schmidt numbers of CO_2 and DMS at the *in situ* sea surface temperature. Compared to normalizing both DMS and CO_2 to Sc=660, this approach has the advantage of correcting only k_{DMS}, with no correction to k_{CO2}. The *Sc* correction for DMS should be reasonably accurate, assuming that the bubble-mediated transfer for the more soluble DMS is relatively small.

On the Knorr_11 cruise, the variability in sea surface temperature was small ($1\sigma = \pm 1°C$). As a result, there is little difference in the variability or wind speed dependence of *Sc*-corrected k_{CO2} compared to k_{CO2} at the *in situ* temperature (Figure 5 vs. Figure ~~S1~~ S5 in Supplemental information). In Section 3.4, the relationship between CO_2 and DMS gas transfer velocities and wind speed is examined using $k_{DMS,Sc}$ and kCO_2.

2.3 Calculation of k_{bub,CO_2}

The flux of a water-side controlled gas ~~transfer velocity (k_w) is comprised~~ is equal to the sum of the interfacial flux and the bubble-mediated flux. For gases with significant air/sea disequilibrium these processes are often considered as parallel transfer velocities, i.e. ~~transfer mechanisms, which operate in parallel,~~ total transfer velocity ~~i.e.~~ $k_w = k_{int} + k_{bub}$. See Woolf

(1997) for a more complete discussion of bubble-mediated transfer for gases close to ocean/atmosphere equilibrium. We assume that turbulence and diffusive mixing at the sea surface operate similarly upon the interfacial air/sea transfer of CO_2 and DMS (i.e. $k_{int,CO2} = k_{int,DMS}$), given appropriate normalization for the differences in molecular diffusivity. Observed differences between $k_{DMS,Sc}$ and k_{CO_2} should therefore be a measure of the difference between the bubble-mediated contributions to DMS and CO_2 gas transfer:

$$\Delta k_w = k_{bub,CO_2} - k_{bub,DMS} \qquad \textit{Equation 5}$$

Strictly speaking, Equation 5 should also account for the influence of bubble overpressure, which alters the gas flux due to bubbles when the concentration gradient is into the ocean. The extra pressure on the gas in the bubbles is calculated following Woolf (1997): $\Delta = (U_{10}/U_i)^2$ % where U_i is the wind speed at which the supersaturation of a particular gas equals 1% (49 m s^{-1} in the case of CO_2). A high wind speed (20 m s^{-1}) gives Δ = 0.167%, which would lead to only a ~2% enhancement of the CO_2 flux when the air/sea concentration gradient is 30 ppm (minimum for this study) and into the ocean. The magnitude of this effect would be larger for gases less soluble than CO_2 but we are able to ignore it for the purposes of this study.

k_{bub,CO_2} and $k_{bub,DMS}$ are related by the influence of solubility and diffusivity upon bubble-mediated transfer. We parameterize this relationship simply as $k_{bub,DMS} = f.k_{bub,CO_2}$. Substitution into Equation 5~~6~~ yields:

$$k_{bub,CO_2} = \frac{\Delta k_w}{1 - f} \qquad \textit{Equation 6}$$

The value of *f* depends on seawater temperature and the complex dynamics of bubble formation and cycling (size distributions, surfactants, etc.). At the mean SST encountered in this study (9.8°C), the bubble gas transfer models of Woolf (Woolf, 1997) and Asher (Asher and Wanninkhof, 1998; Asher et al., 2002) yield values for *f* of 0.14 and 0.28~~7~~, respectively (see Supplemental information for model equations).

2.4 Sea surface imaging

Whitecap areal fraction was measured using images of the sea surface recorded with a digital camera (5 mega pixel Arecont Vision, 16 mm focal length lens) mounted 14.6 m above the

ocean surface at an angle of ~75° from the nadir. Image footprints represent ~7600 m^2 of sea surface. Images were collected at a sample period of about 1 second and post-processed for whitecap fraction according to the Automated Whitecap Extraction algorithm method (Callaghan and White, 2009). More detail on the methodology, camera exposure settings and data comparability are provided in the Supplemental information. Images were further processed to distinguish whitecap pixels as either stage A or stage B whitecaps by applying a spatial separation technique (Scanlon and Ward, 2013). The whitecap fraction measurements were averaged in the same way as the gas transfer velocities (i.e. time-averaged mean values as well as 2 m s^{-1} wind speed bins).

3 Results

3.1 Cruise location and environmental conditions

This study took place in the summertime North Atlantic (June 24 – July 18, 2011; DOY 175-199), departing and returning to Woods Hole, MA. Most of the data were collected north of 50°N, including the occupation of four 24-36 hr stations – ST181, ST184, ST187 and ST191 (Figure~~s~~ 1~~ & 2~~). The cruise track was designed to sample regions with high biological productivity and phytoplankton blooms, with large air/sea concentration differences for CO_2 and DMS. The cruise meteorology and physical oceanography is discussed in detail by (Bell et al., 2013). A series of weather systems travelling from West to East passed over the region during the cruise. Wind speeds ranged from ~1 to 22 m s^{-1}, with strongest winds during the frontal passages at stations ST184 and ST191 (Figure 1b). Atmospheric boundary layer stability was close to neutral for most of the cruise ($|z/L| < 0.07$; 75% of the time), with infrequent stable conditions ($z/L > 0.05$; <8% of the time, Figure 1a). There was no evidence that the stable periods affected the flux measurements (Bell et al., 2013). Whitecap areal fraction increased up to a maximum of ~0.06 in response to high wind speeds (Figure 1b).

3.2 Whitecaps

Whitecaps were observed during Knorr_11 when wind speeds exceeded 4.5 m s^{-1}, a typical wind speed threshold for whitecap formation in the open ocean (Callaghan et al., 2008; Schwendeman and Thomson, 2015). Whitecap areal fraction is a strong, non-linear function of wind speed (Figure 2~~3~~a). The whitecap vs. wind speed relationship for Knorr_11 is similar in shape~~, but considerably lower than~~ to recently~~ previously~~ published, wind speed-based

whitecap parameterisations (Callaghan et al., 2008; Schwendeman and Thomson, 2015). At intermediate wind speeds the Knorr_11 whitecap data are ~~as much as an order of magnitude~~ lower than the parameterisations (Figure 2~~3~~a).

Total whitecap coverage is a function of (i) active 'stage A whitecaps' (W_A) produced from recent wave breaking and (ii) maturing 'stage B whitecaps' (W_B) that are decaying foam from previous breakers. The Stage A whitecap fraction data is highly variable at ~11 m s^{-1} wind speeds (Figure 2~~3~~b), which is driven by the difference in the wind-wave conditions during Knorr_11 (~~ST184 vs ST191, Figure 4a~~see discussion in Supplemental information). ~~Stage A whitecap fraction data does not show the same differences between ST184 and ST191 when plotted against the dimensionless Reynolds number, R_H, which describes breaking waves using Knorr_11 measurements of significant wave height (Zhao and Toba, 2001). The relationship between Stage A whitecap fraction and R_H is more scattered when Stage A whitecaps are below ~10^{-4} (Figure 4b). Wave development and steepness (slope) influence the likelihood of breaking waves. Breaking waves are more closely associated with steep, young waves. At a given wind speed and wave height, older, swell-dominated waves do not produce as many stage A whitecaps compared to young wave systems (Sugihara et al., 2007; Callaghan et al., 2008).~~

3.3 Concentrations, fluxes and gas transfer velocities

Seawater pCO_2 was consistently lower than the overlying atmosphere throughout the study region due to biological uptake (Figure 3a~~1c~~). As a result, the air/sea concentration difference (ΔpCO_2) was large and always into the ocean, with ΔpCO_2 <-45 ppm for more than 80% of the measurements. Periods with particularly enhanced ΔpCO_2 into the ocean were during the transit between ST181 and ST184 (ΔpCO_2 as large as -120 ppm) and during ST191 (ΔpCO_2 consistently -75 ppm).

Seawater DMS levels were much higher than atmospheric levels, reflecting the biogenic sources in seawater and the relatively short atmospheric lifetime (~1 day; Kloster et al., 2006). The largest air/sea DMS concentration differences (ΔDMS) of 6-12 ppb were observed during DOY 185-190 (Figure 4~~2~~a). The ΔDMS and ΔpCO_2 did not co-vary (Spearman ρ = 0.11, n=918, p<0.001). This is not surprising because, although seawater DMS and CO_2 signals are both influenced by biological activity, they are controlled by different processes. Seawater CO_2 levels reflect the net result of community photosynthesis and respiration, while DMS

627 production is related to metabolic processes that are highly species-dependent (Stefels et al.,
628 2007).

629 CO_2 fluxes (F_{CO2}) were generally into the ocean, as expected given the direction of the air/sea
630 concentration difference (Figure 3b~~1d~~). The variability in F_{CO2} observed on this cruise reflects
631 dependence on both wind speed and ΔpCO_2. For example, during DOY182 air-to-sea CO_2
632 fluxes increase due to a gradual increase in ΔpCO_2 with fairly constant wind speed. More
633 commonly, ΔpCO_2 was fairly constant and variability in F_{CO2} reflected changes in wind speed.
634 For example, from DOY 185-187 wind speeds gradually declined from ~10 to 5 m s^{-1} with a
635 concurrent decline in F_{CO2}. DMS eddy covariance fluxes were always out of the ocean. Ten
636 minute averaged DMS fluxes (F_{DMS}) clearly show the influence of ~~both~~ ΔDMS (e.g. DOY 188)
637 and wind speed (e.g. DOY 184).

638 Gas transfer velocities of CO_2 and DMS from this cruise exhibit two systematic differences: i)
639 k_{DMS} values are generally lower than k_{CO_2}, particularly during episodes of high wind speed;
640 and ii) k_{CO_2} is characterized by much larger scatter than k_{DMS}. We attribute the large scatter in
641 k_{CO_2} to the greater random uncertainty associated with the eddy covariance measurement of
642 air/sea CO_2 fluxes compared to those of DMS. As shown by Miller et al. (2010), the analytical
643 approach used in this study (dried air, closed path LI7500) has sufficient precision to
644 adequately resolve the turbulent fluctuations in atmospheric ~~p~~CO_2 associated with the surface
645 flux over most of the cruise (ΔpCO_2 < -30 ppm). The scatter in the CO_2 flux measurements is
646 more likely due to environmental variability resulting from fluctuations in boundary layer CO_2
647 mixing ratio arising from horizontal and/or vertical transport unrelated to air/sea flux (Edson
648 et al., 2008; Blomquist et al., 2014). These effects likely have a much smaller effect on air/sea
649 DMS fluxes, because the air/sea DMS concentration difference is always much larger than the
650 mean atmospheric DMS concentration (due to the short atmospheric lifetime of DMS). For
651 example, a ΔpCO_2 of 100 ppm at a wind speed of 10 m s^{-1} will produce turbulent fluctuations
652 that are ~0.02% of the background CO_2 on average. In contrast, a typical seawater DMS
653 concentration (2.6 nM) at a wind speed of 6 m s^{-1} generates fluctuations ~~of~~ that are 20% of the
654 background (Table 1; Blomquist et al., 2012). Thus, F_{CO2} measurements are highly sensitive
655 to small fluctuations in background CO_2 and the relative uncertainty is expected to be much
656 larger than that for F_{DMS}.

3.4 Comparison of k_{CO_2} and $k_{DMS,Sc}$

The differences between CO_2 and DMS gas transfer velocities observed in the time series are also evident when the data are examined as a function of wind speed. From the 10-minute averaged data, it is clear that k_{CO_2} is greater than k_{DMS} and has a stronger wind speed-dependence over most of the wind speed range (Figure 5a,b). These broad trends are also easily seen in longer time-averaged data. Flux and ΔC measurements were averaged into ~~4~~2 hour periods (minimum of 3 flux intervals per 2~~4~~ hour period), which reduced the scatter in F_{CO2} while preserving the temporal variability (see Figure ~~S3~~S7 in Supplemental information). Gas transfer velocities were then recalculated from the ~~4~~ 2 hour averaged data. 10-minute k_{CO_2} and $k_{DMS,Sc}$ data were also averaged into 2 m s^{-1} wind speed bins, with a minimum of five~~5~~ 10~~ten~~ minute periods per bin. The 2~~4~~ hour averaged data and the wind speed binned data show k_{CO_2} and $k_{DMS,Sc}$ diverging at intermediate wind speeds, differing by a factor of roughly two at 10 m s^{-1} (Figure 5c,d).

DMS gas transfer velocities on this cruise exhibit complex behaviour at intermediate to high wind speeds, as discussed in Bell et al. (2013). $k_{DMS,Sc}$ increases linearly with wind speed up to ~11 m s^{-1} (Figure 5). Under the sustained high wind, high wave conditions encountered during ST191, the wind speed-dependence of $k_{DMS,Sc}$ was lower than expected, with a slope roughly half that of the rest of the cruise data. This effect was not observed at ST184 – for detailed discussion, see Bell et al. (2013). Such coherent spatial-temporal variation means that wind speed bin averaging of the higher wind speed $k_{DMS,Sc}$ may mask real variability in the relationship with wind speed. Relationships developed from wind speed bin-averaged gas transfer data should be interpreted with caution, especially when it comes to developing generalizable air/sea gas transfer models.

The Knorr_11 k_{CO_2} data also demonstrate a clear wind speed dependence (Figure 5). The NOAA COARE model for CO_2 has been tuned to previous eddy covariance flux measurements (McGillis et al., 2001), with bubble-mediated transfer determining the non-linear relationship with wind speed (Fairall et al., 2011). There is reasonable agreement between the COARE model gas transfer velocity predictions and the Knorr_11 k_{CO_2} data ~~until~~ up to ~11 m s^{-1} wind speed. Above 11 m s^{-1}, the COARE model over predicts k_{CO_2}. This could be interpreted as indicating high wind speed suppression of gas transfer for CO_2 as observed for DMS (as

discussed by Bell et al., 2013). However, it is important to note that the number of high wind speed (>15 m s^{-1}) gas transfer measurements in this study is limited to 9 hours and 16 hours of data for DMS and CO2 respectively. Much more data are needed in order to firmly establish the high wind speed behaviour.

The COAREG 3.1 model parameterizes interfacial gas transfer by scaling to *Sc* and friction velocity and estimates bubble-mediated gas transfer following Woolf (1997). The lower solubility of CO_2 leads to enhanced gas transfer relative to that of DMS at high wind speeds where bubble transport is significant (Fairall et al., 2011). There is good agreement between the COAREG model gas transfer velocity predictions and the Knorr_11 k_{CO_2} and k_{DMS} data until ~11 m s^{-1} wind speed.

Earlier in this paper we introduced the quantity Δk_w as an observational measure of the difference in gas transfer velocities of CO_2 and DMS (Section 2.3, ~~e~~Equation 6). The relationship between Δk_w and wind speed is positive and shows no systematic differences related to temporal variability (Figure 6). Sea surface temperature (SST) is indicated by symbol size. Some of the scatter in Figure 6 could be driven by changes in *Sc* due to SST variability. Nearly all of the data in Figure 6 ~~is~~ are from periods when SST was relatively constant (9.7~~8~~±1.1~~0~~°C). Many of the k_{CO_2} data with warm seawater (i.e. ST181, SST > 12°C) were rejected by our quality control criteria (see Appendix A.3). These data were collected when wind speeds were low, which resulted in small CO_2 fluxes with large variability at low frequencies. Of the periods with SST > 12°C that passed the quality control criteria, the majority contributed fewer data within a 2~~4~~ hour averaging period than the minimum threshold (three 10~~-~~-minute averaged data points). ~~Only one 4 hour period passed the thresholds for flux quality control and number of points, and this was associated with the most negative Δk_w value.~~

4 Discussion

The bubble-mediated component of gas transfer is a strong function of wind speed and breaking waves. Previous estimates of bubble-mediated air/sea gas exchange have ~~been based on~~used data from laboratory experiments (Keeling, 1993; Asher et al., 1996; Woolf, 1997). The differences between gas transfer velocities for DMS and CO_2 provide a unique way to constrain the importance of bubble-mediated transfer under natural conditions. This study shows that Δk_w is near zero (< 4.5 cm hr^{-1}) at ~~very~~ low wind speeds ($U_{10} \leq 4.5$ m s^{-1}), which is consistent

with the wind speed at which whitecap fraction becomes significant (W_T> 10^{-5}, Figure 23a). Above 4.5 m s^{-1}, Δk_w increases non-linearly, consistent with an increase in bubble-mediated CO_2 transfer associated with wave breaking. The relationship between Δk_w and wind speed is non-linear, and ~~the quadratic~~a power law wind speed-dependence yields a good fit (R^2 = 0.6677; Figure 6):

$$\Delta k_w = 0.157 0.177 U_{10}^{2} - 0.535 U_{10}^{1.928} + 4.289 \qquad \textit{Equation 7}$$

The functional form of this relationship is qualitatively consistent with those found between U_{10} and breaking waves/wave energy dissipation (Melville and Matusov, 2002) and U_{10} vs. whitecap areal fraction (e.g. Callaghan et al., 2008; Schwendeman and Thomson, 2015). Bubble-mediated gas transfer is the only viable explanation for the magnitude and wind-speed dependence of Δk_w. The only alternative explanation would require a large systematic bias in the measurement of relative gas transfer velocities of DMS and CO_2. There are no obvious candidates for such biases.

During strong wind/large wave conditions, the Knorr_11 data suggest that bubble-mediated exchange is a dominant contributor to the total transfer of CO_2. For example, when wind speeds were 11-12 m s^{-1}, Δk_w was about 50% of the total CO_2 gas transfer (k_{CO_2}). A significant contribution by bubbles to the total gas transfer velocity means that bubble-mediated exchange must be included and adequately parameterised by gas transfer models. The Schmidt number (*Sc*) normalisation (Equation 4) assumes that the gas transfer velocity is purely interfacial. An alternative normalisation (involving *Sc* and solubility) is required when bubble-mediated transfer is significant. Our data suggest that the current *Sc* normalisation should be applied with caution to gas transfer data for different solubility gases at wind speeds greater than 10 m s^{-1}.

If Δk_w reflects the difference between the bubble-mediated contribution to the transfer of CO_2 and DMS, one would expect Δk_w to correlate with wave-breaking, and hence with the areal coverage of whitecaps. Breaking waves generate plumes of bubbles (Stage A whitecaps, W_A), which then rise to the surface and persist for a short period as foam (Stage B whitecaps, W_B). Almost all whitecap measurements represent the fraction of the sea surface that is covered by bubble plumes and/or foam i.e. $W_T = W_A + W_B$. Δk_w is positively correlated with both W_T (Spearman ρ = 0.6581, n=4332, p<0.001) and W_A (Spearman ρ = 0.7482, n=3226, p<0.001) (Figure 7a,b). These correlations are approximately the same strength as the correlation between Δk_w and wind speed (Spearman ρ = 0.7383, n=8855, p<0.001). The functional form

of the relationship between Δk_w and whitecap areal extent appears to be linear for $W_T > 0.005$. However, the Knorr_11 dataset is small and quite scattered, particularly when $W_T < 0.005$. More data are required to fully test the validity of whitecap areal fraction as a proxy for bubbles and bubble-mediated exchange.

Observations of the decaying white cap signal (W_B) suggest that the persistence of surface foam is related to both bubble plume depth (deeper bubble plumes take longer to degas) and sea surface chemistry (Callaghan et al., 2013). As measured here, W_B is approximately an order of magnitude larger than W_A and thus dominates the W_T signal. It is often assumed that gas exchange takes place in bubble plumes formed by active wave breaking (i.e. W_A), while W_B may vary widely due to surfactant concentration with little or no impact upon bubble-mediated gas exchange (e.g. Pereira et al., 2016). In this case, Δk_w should be more strongly correlated with W_A than W_B or W_T. The Knorr_11 data do not suggest that W_A is an improvement upon either W_T or even wind speed as a measure of bubble mediated exchange. This may be because whitecaps do not fully represent the bubbles facilitating gas exchange as these may dissolve before they reach the sea surface. Alternatively, W_T and W_A may be equally good (or poor) proxies for bubbles because: (i) surfactant activity was either insignificant~~minimal~~ or sufficiently invariant in the study region (despite high biological productivity) ~~such~~ that W_B does not confound the relationship between W_T and W_A; (ii) W_A is no better than W_T at representing the volume of air entrained by breaking waves; and/or (iii) bubbles residing at the surface (i.e. W_B) continue to contribute to gas transfer (Goddijn-Murphy et al., 2016).

As shown earlier, the bubble-mediated contribution to gas transfer (k_{bub,CO_2}) can be obtained from Δk_w using information from mechanistic bubble gas transfer models (f, see Section 2.3). The k_{bub,CO_2} datasets derived from the Knorr_11 data using the Asher (Asher and Wanninkhof, 1998; Asher et al., 2002) and Woolf (Woolf, 1997) models differ by about 15% (Figure 8). The field-based estimates of k_{bub,CO_2} can also be compared to model-only estimates for the Knorr_11 conditions using the Asher and Woolf models. Both models are based on total whitecap areal fraction, W_T. A non-linear fit of the Knorr_11 W_T and wind speed measurements ($W_T = 1.9 \times 10^{-6} U_{10n}^{3.36}$) was used to drive both models (Figure 8). Asher et al. (2002) is based on laboratory tipping bucket gas evasion experiments (Asher et al., 1996) and the model was then adjusted to represent the flux of CO_2 into the ocean (invasion). Woolf (1997) scaled a single bubble model to the open ocean based on laboratory experiments.

779 Both models significantly underestimate k_{bub,CO_2} at wind speeds below about 11 m s^{-1}. At higher
780 wind speeds, the Asher et al. (2002) model increases rapidly with wind speed to agree ~~slightly~~
781 better with the Knorr_11 data. In contrast, Woolf (1997) consistently underestimates k_{bub,CO_2}
782 at all wind speeds. Both k_{bub,CO_2} models depend on the choice of wind speed-whitecap
783 parameterisation. Using the Schwendeman and Thomson (2015) whitecap parameterisation
784 instead of the Knorr_11 best fit makes some difference to the model output, but not enough to
785 adequately fit to the data (Figure 8). A 'dense plume model' was also developed by Woolf et
786 al. (2007) to take account of the interaction of a bubble plume with the interstitial water
787 between bubbles. This model yields estimates of k_{bub,CO_2} that are even lower than the original
788 Woolf (1997) 'single bubble model' (data not shown).

789 It is likely that the Knorr_11 cruise data will be compared with estimates of k_{bub,CO_2} derived
790 from future field campaigns, which will be conducted under different environmental
791 conditions. Our k_{bub,CO_2} data is at *in situ* seawater temperature (~10°C) and thus *in situ* CO_2
792 solubility (α=1.03) and diffusivity (*Sc*=1150). We use the Asher et al. (2002) and Woolf (1997)
793 bubble models to make estimates of k_{bub,CO_2} normalised to a standard seawater temperature of
794 20°C ($k_{bub,CO_2,20°C}$, where α=0.78 and *Sc*=666). The 24 ~~4~~ hour averaged Knorr_11 cruise data,
795 including estimates of Δk_w, k_{bub,CO_2} and $k_{bub,CO_2,20°C}$, are provided in Supplemental Table S1.

796 The approach used in this study to estimate Δk_w and k_{bub,CO_2} from the Knorr_11 field data
797 neglects the effect of sea surface skin temperature and CO_2 chemical enhancement. Skin
798 temperature is typically only a few tenths of a degree less than bulk seawater under the
799 conditions encountered in this study (Fairall et al., 1996). The impact upon k_{CO_2} due to skin
800 temperature effects on CO_2 solubility and carbonate speciation is likely on the order of 3%
801 (Woolf et al., 2016). There is a chemical enhancement of the CO_2 flux due to ionization at the
802 sea surface (Hoover and Berkshire, 1969). The effect on k_{CO_2} has been estimated to be up to
803 about 8% at a wind speed of 4-6 m s^{-1} (Wanninkhof and Knox, 1996), which amounts to a
804 maximum impact of a few cm hr^{-1}. By neglecting these effects we have slightly overestimated
805 Δk_w and k_{bub,CO_2}, but the magnitude of these corrections would be small relative to the
806 environmental scatter or measurement uncertainty.

5 Conclusions

The Knorr_11 concurrent measurements of DMS and CO_2 gas transfer velocities show significant differences in gas transfer between the two gases at intermediate-high wind speeds. These data indicate that: i) bubble-mediated gas transfer becomes significant for CO_2 at or above the threshold for wave-breaking; and ii) the wind speed-dependence is non-linear, with a similar functional form to proposed relationships predicting whitecap areal extent from wind speed. However, existing models of bubble-mediated gas transfer using the Knorr_11 *in situ* observations of whitecap fraction significantly underestimate the importance of this process.

There are a number of assumptions behind model estimates of bubble-mediated gas exchange (Goddijn-Murphy et al., 2016). Model bias can be crudely split into: i) uncertainties in the scaling of whitecap fraction to the bubble population (e.g. using Cipriano and Blanchard, 1981); and ii) the relationship between gas exchange and bubble properties, which are predicted as a function of air entrainment into the surface ocean by a breaking wave, bubble injection depth, size distribution and mobility through the water (a function of surface cleanliness and surfactants). The underestimation of bubble-mediated CO_2 gas transfer by both models is particularly apparent at low-intermediate wind speeds and low whitecap fraction. This could indicate that either bubble production during microscale breaking is an important process for gas transfer or the relationship between whitecap fraction and the bubble population is poorly constrained.

In summary, the approach of using simultaneous measurements of multiple gases with different solubility appears to be a viable way to constrain the magnitude of bubble-mediated gas transfer. Analysis of additional sparingly soluble gases, such as methane or oxygenated hydrocarbons would further strengthen this approach. A much larger data set, under a wider range of oceanographic conditions is certainly needed. In particular, it would be useful to examine DMS and CO_2 gas transfer velocities in ocean regions with different temperatures, where the solubility of each gas is significantly different from this study.

Appendix A

A.1 Seawater CO_2 and DMS measurements

Seawater CO_2 and DMS were monitored in the supply of seawater pumped continuously through the ship from an intake on the bow located 6 m below the sea surface. CO_2 was equilibrated with air in a recirculating showerhead-type system. Alternate air and water side pCO_2 were each measured for 5 min by the same Infrared Gas Analyser (IRGA). Seawater DMS was equilibrated with DMS-free air in a tubular porous membrane equilibrator, operated in a single-pass, counterflow mode. DMS was measured at 1 Hz using chemical ionization mass spectrometry and bin-averaged at 1 minute intervals (UCI miniCIMS; Saltzman et al., 2009). DMS was calibrated by continuously pumping an internal standard of tri-deuterated, DMS (d3-DMS) into the seawater flow just before the equilibrator. Details of the methods and instrumentation used for equilibration and detection of seawater DMS are described in Saltzman et al. (2009).

A.2 Mast-mounted instrumentation and data acquisition

The eddy covariance ~~setup~~ system was mounted 13.6 m above the sea surface on the bow mast. Platform angular rates and accelerations were measured by two Systron Donner Motion Pak II (MPII) units. Three dimensional winds and sonic temperature were measured by two Campbell CSAT3 sonic anemometers. Air sampling inlets for DMS and CO_2 were located at the same height as the anemometers and within 20 cm of the measurement region. GPS and digital compass output were digitally logged at 1 Hz. Winds were corrected for ship motion and orientation as described in Miller et al. (2008) and Landwehr et al. (2015). The eddy covariance data streams were logged in both analog and digital format as described in Bell et al. (2013) ~~and Miller et al., In Prep~~.

A.3 High frequency atmospheric DMS and CO_2 measurements

Atmospheric DMS measurements were made at 10 Hz using an atmospheric pressure chemical ionisation mass spectrometer located in a lab van (UCI mesoCIMS; Bell et al. (2013)). Air was drawn to the instrument through a 28 m long ½ in OD Teflon tube. A subsample of the air stream was passed through a Nafion drier prior to entering the mass spectrometer. The

862 measurement was calibrated using an internal gas standard of tri-deuterated DMS added to the
863 inlet (see Bell et al., 2013).

864 Atmospheric CO_2 measurements were made on air drawn at 8 L min^{-1} through a filtered inlet
865 (90 mm diameter with 1 micron pore size, Savillex) near the sonic anemometers on the bow
866 mast, through 5 m of 5.9 mm ID polyethylene-lined Dekabon tubing to two fast-response
867 CO_2/H_2O IRGAs in an enclosure on the bow mast. The IRGAs were open-path style sensors
868 (LI7500, Licor Inc.) converted to a closed-path configuration (see Miller et al., 2010) and were
869 plumbed in series. A Nafion multi-tube membrane drier (PD-200T, PermaPure) with 6 L min^{-1}
870 dry air counter flow was installed between the two IRGAs such that the upstream IRGA
871 sampled undried air and the downstream IRGA sampled the same air after drying. This
872 technique removes 97% of the Webb Correction from the measured CO_2 flux (first shown by
873 Miller et al. (2010) and confirmed by Landwehr et al. (2014)).

874 The air flow through both the CO_2 and DMS inlets was fully turbulent (Re > 10,000). The inlets
875 used in this study introduced a small delay (Δt = 2.2 s for DMS, Δt = 1.2 s for CO_2) between
876 measured wind and atmospheric measurements, as well as minor loss of covariance at high
877 frequencies (<5%). The methods used to estimate the delay and loss of flux are given in Bell
878 et al. (2013).

879 Eddy covariance fluxes were computed for DMS and CO_2 as F_{DMS} or $F_{CO2} = \sigma_{air} \langle w'c' \rangle$

880 where σ_{air} is the dry air density, w' is the fluctuation in vertical winds and c' is the delay-
881 adjusted fluctuation in gas concentration. Average covariance fluxes were processed in 10
882 minute and 9.5 minute intervals for DMS and CO_2, respectively (hereafter referred to as 10
883 minute intervals). Momentum and sensible heat fluxes were also computed for 10 minute
884 intervals (see Bell et al., 2013).

885 Sampling intervals with a mean wind direction relative to the bow of >90° were excluded from
886 the final data set. CO_2 fluxes were also excluded from intervals when either: i) relative wind
887 direction changed excessively (SD > 10°); ii) relative wind speed was low (< 1 m s^{-1}); or iii)
888 ΔCO_2 was low (< |30| ppm). DMS and CO_2 fluxes were quality controlled for excessive low
889 frequency flux as described in the Supplemental information of Bell et al. (2013). These quality
890 control criteria excluded 62% of the intervals for CO_2 and 55% for DMS and significantly
891 reduced the scatter in the data.

892

Acknowledgements. We thank the Captain and crew of the R/V Knorr and the Woods Hole Marine Department for their assistance in carrying out this cruise. Funding for this research was provided by the NSF Atmospheric Chemistry Program (AGS-0851068, -0851472, -0851407 and -1134709) and the NSF Independent Research and Development program. A. C. acknowledges support from a Royal Society Shooter International Fellowship and from the National Science Foundation under grant OCE-1434866. B. W. acknowledges support from Science Foundation Ireland under grant 08/US/I1455 and from the FP7 Marie Curie Reintegration programme under grant 224776. We are grateful for constructive comments from our reviewers (Byron Blomquist, Ian Brooks and Bill Asher), which helped improve the paper. This study is a contribution to the international Surface Ocean Lower Atmosphere Study (SOLAS) programme.

References

Asher, W. E., Karle, L. M., Higgins, B. J., Farley, P. J., Monahan, E. C., and Leifer, I. S.: The influence of bubble plumes on air-seawater gas transfer velocities, J Geophys Res-Oceans, 101, 12027-12041, 1996.

Asher, W. E., and Wanninkhof, R.: The effect of bubble-mediated gas transfer on purposeful dual-gaseous tracer experiments, Journal of Geophysical Research: Oceans, 103, 10555-10560, 10.1029/98jc00245, 1998.

Asher, W. E., Edson, J., McGillis, W., Wanninkhof, R., Ho, D. T., and Litchendor, T.: Fractional area whitecap coverage and air-sea gas transfer velocities measured during GasEx-98, in: Gas Transfer at Water Surfaces, American Geophysical Union, 199-203, 2002.

Bell, T. G., de Bruyn, W., Miller, S. D., Ward, B., Christensen, K., and Saltzman, E. S.: Air/sea DMS gas transfer in the North Atlantic: evidence for limited interfacial gas exchange at high wind speed, Atm Chem Phys, 13, 11073-11087, 2013.

Bell, T. G., de Bruyn, W., Marandino, C. A., Miller, S. D., Law, C. S., Smith, M. J., and Saltzman, E. S.: Dimethylsulfide gas transfer coefficients from algal blooms in the Southern Ocean, Atm Chem Phys, 15, 1783-1794, 10.5194/acp-15-1783-2015, 2015.

Blomquist, B. W., Fairall, C. W., Huebert, B. J., Kieber, D. J., and Westby, G. R.: DMS sea-air transfer velocity: Direct measurements by eddy covariance and parameterization based on the NOAA/COARE gas transfer model, Geophysical Research Letters, 33, art. no.-L07601, 10.1029/2006gl025735, 2006.

Blomquist, B. W., Fairall, C. W., Huebert, B. J., and Wilson, S. T.: Direct measurement of the oceanic carbon monoxide flux by eddy correlation, Atmos Meas Tech, 5, 3069-3075, 10.5194/amt-5-3069-2012, 2012.

Blomquist, B. W., Huebert, B. J., Fairall, C. W., Bariteau, L., Edson, J. B., Hare, J. E., and McGillis, W. R.: Advances in air-sea CO_2 flux measurement by eddy correlation, Boundary-Layer Meteorology, 152, 245-276, 10.1007/s10546-014-9926-2, 2014.

Callaghan, A. H., de Leeuw, G., Cohen, L., and O'Dowd, C. D.: Relationship of oceanic whitecap coverage to wind speed and wind history, Geophysical Research Letters, 35, L23609, 10.1029/2008gl036165, 2008.

Callaghan, A. H., and White, M.: Automated processing of sea surface images for the determination of whitecap coverage, Journal of Atmospheric and Oceanic Technology, 26, 383-394, 10.1175/2008jtecho634.1, 2009.

Callaghan, A. H., Deane, G. B., and Stokes, M. D.: Two regimes of laboratory whitecap foam decay: Bubble-plume controlled and surfactant stabilized, Journal of Physical Oceanography, 43, 1114-1126, 10.1175/Jpo-D-12-0148.1, 2013.

Carpenter, L. J., Archer, S. D., and Beale, R.: Ocean-atmosphere trace gas exchange, Chem Soc Rev, 41, 6473-6506, 10.1039/c2cs35121h, 2012.

Cipriano, R. J., and Blanchard, D. C.: Bubble and aerosol spectra produced by a laboratory 'breaking wave', Journal of Geophysical Research: Oceans, 86, 8085-8092, 10.1029/JC086iC09p08085, 1981.

Dacey, J. W. H., Wakeham, S. G., and Howes, B. L.: Henry's law constants for dimethylsulfide in fresh water and seawater, Geophysical Research Letters, 11, 991-994, 1984.

Edson, J. B., DeGrandpre, M. D., Frew, N. M., and McGillis, W. R.: Investigations of air-sea gas exchange in the CoOP Coastal Air-Sea Chemical Exchange Project, Oceanography, 21, 34-45, http://dx.doi.org/10.5670/oceanog.2008.03, 2008.

Fairall, C. W., Bradley, E. F., Godfrey, J. S., Wick, G. A., Edson, J. B., and Young, G. S.: Cool-skin and warm-layer effects on sea surface temperature, J Geophys Res-Oceans, 101, 1295-1308, 10.1029/95jc03190, 1996.

Fairall, C. W., Yang, M., Bariteau, L., Edson, J. B., Helmig, D., McGillis, W., Pezoa, S., Hare, J. E., Huebert, B., and Blomquist, B.: Implementation of the Coupled Ocean-Atmosphere Response Experiment flux algorithm with CO2, dimethyl sulfide, and O3, J Geophys Res-Oceans, 116, C00F09, 10.1029/2010jc006884, 2011.

Goddijn-Murphy, L., Woolf, D. K., and Marandino, C.: Space-based retrievals of air-sea gas transfer velocities using altimeters: Calibration for dimethyl sulfide, J Geophys Res-Oceans, 117, 10.1029/2011jc007535, 2012.

Goddijn-Murphy, L., Woolf, D. K., Callaghan, A. H., Nightingale, P. D., and Shutler, J. D.: A reconciliation of empirical and mechanistic models of the air-sea gas transfer velocity, Journal of Geophysical Research: Oceans, 121, 818-835, 10.1002/2015jc011096, 2016.

Hoover, T. E., and Berkshire, D. C.: Effects of hydration on carbon dioxide exchange across an air-water interface, Journal of Geophysical Research, 74, 456-464, 1969.

Huebert, B. J., Blomquist, B. W., Hare, J. E., Fairall, C. W., Johnson, J. E., and Bates, T. S.: Measurement of the sea-air DMS flux and transfer velocity using eddy correlation, Geophysical Research Letters, 31, L23113, 10.1029/2004gl021567, 2004.

Keeling, R. F.: On the role of large bubbles in air-sea gas exchange and supersaturation in the ocean, Journal of Marine Research, 51, 237-271, 10.1357/0022240933223800, 1993.

Kloster, S., Feichter, J., Reimer, E. M., Six, K. D., Stier, P., and Wetzel, P.: DMS cycle in the marine ocean-atmosphere system - a global model study, Biogeosciences, 3, 29-51, 2006.

Landwehr, S., Miller, S. D., Smith, M. J., Saltzman, E. S., and Ward, B.: Analysis of the PKT correction for direct CO_2 flux measurements over the ocean, Atm Chem Phys, 14, 3361-3372, 10.5194/acp-14-3361-2014, 2014.

Landwehr, S., O'Sullivan, N., and Ward, B.: Direct flux measurements from mobile platforms at sea: Motion and airflow distortion corrections revisited, Journal of Atmospheric and Oceanic Technology, 32, 1163-1178, 10.1175/jtech-d-14-00137.1, 2015.

Le Quéré, C., Moriarty, R., Andrew, R. M., Peters, G. P., Ciais, P., Friedlingstein, P., Jones, S. D., Sitch, S., Tans, P., Arneth, A., Boden, T. A., Bopp, L., Bozec, Y., Canadell, J. G., Chini, L. P., Chevallier, F., Cosca, C. E., Harris, I., Hoppema, M., Houghton, R. A., House, J. I., Jain, A. K., Johannessen, T., Kato, E., Keeling, R. F., Kitidis, V., Klein Goldewijk, K., Koven, C., Landa, C. S., Landschützer, P., Lenton, A., Lima, I. D., Marland, G., Mathis, J. T., Metzl, N., Nojiri, Y., Olsen, A., Ono, T., Peng, S., Peters, W., Pfeil, B., Poulter, B., Raupach, M. R., Regnier, P., Rödenbeck, C., Saito, S., Salisbury, J. E., Schuster, U., Schwinger, J., Séférian, R., Segschneider, J., Steinhoff, T., Stocker, B. D., Sutton, A. J., Takahashi, T., Tilbrook, B., van der Werf, G. R., Viovy, N., Wang, Y. P., Wanninkhof, R., Wiltshire, A., and Zeng, N.: Global carbon budget 2014, Earth System Science Data, 7, 47-85, 10.5194/essd-7-47-2015, 2015.

Liss, P. S., and Slater, P. G.: Flux of gases across the air-sea interface, Nature, 247, 181-184, 1974.

Liss, P. S., and Merlivat, L.: Air-sea gas exchange rates: introduction and synthesis, in: The role of air-sea exchange in geochemical cycling, edited by: Buatmenard, P., Reidel, 113-127, 1986.

Marandino, C. A., de Bruyn, W. J., Miller, S. D., and Saltzman, E. S.: Eddy correlation measurements of the air/sea flux of dimethylsulfide over the North Pacific Ocean, Journal of Geophysical Research-Atmospheres, 112, art. no.-D03301, 10.1029/2006jd007293, 2007.

McGillis, W. R., Dacey, J. W. H., Frew, N. M., Bock, E. J., and Nelson, R. K.: Water-air flux of dimethylsulfide, J Geophys Res-Oceans, 105, 1187-1193, 2000.

McGillis, W. R., Edson, J. B., Hare, J. E., and Fairall, C. W.: Direct covariance air-sea CO_2 fluxes, J Geophys Res-Oceans, 106, 16729-16745, 2001.

Melville, W. K., and Matusov, P.: Distribution of breaking waves at the ocean surface, Nature, 417, 58-63, 2002.

Miller, S. D., Hristov, T. S., Edson, J. B., and Friehe, C. A.: Platform motion effects on measurements of turbulence and air-sea exchange over the open ocean, Journal of Atmospheric and Oceanic Technology, 25, 1683-1694, 10.1175/2008jtecho547.1, 2008.

Miller, S. D., Marandino, C., de Bruyn, W., and Saltzman, E. S.: Air-sea gas exchange of CO_2 and DMS in the North Atlantic by eddy covariance, Geophysical Research Letters, 36, art. no.-L15816, 10.1029/2009gl038907, 2009.

Miller, S. D., Marandino, C., and Saltzman, E. S.: Ship-based measurement of air-sea CO_2 exchange by eddy covariance, Journal of Geophysical Research-Atmospheres, 115, art. no.-D02304, 10.1029/2009jd012193, 2010.

Pereira, R., Schneider-Zapp, K., and Upstill-Goddard, R. C.: Surfactant control of gas transfer velocity along an offshore coastal transect: results from a laboratory gas exchange tank, Biogeosciences, 13, 3981-3989, 10.5194/bg-13-3981-2016, 2016.

Rhee, T. S., Nightingale, P. D., Woolf, D. K., Caulliez, G., Bowyer, P., and Andreae, M. O.: Influence of energetic wind and waves on gas transfer in a large wind-wave tunnel facility, J Geophys Res-Oceans, 112, art. no.-C05027, 10.1029/2005jc003358, 2007.

Saltzman, E. S., King, D. B., Holmen, K., and Leck, C.: Experimental determination of the diffusion coefficient of dimethylsulfide in water, J Geophys Res-Oceans, 98, 16481-16486, 1993.

Saltzman, E. S., de Bruyn, W. J., Lawler, M. J., Marandino, C. A., and McCormick, C. A.: A chemical ionization mass spectrometer for continuous underway shipboard analysis of dimethylsulfide in near-surface seawater, Ocean Science, 5, 537-546, 2009.

Scanlon, B., and Ward, B.: Oceanic wave breaking coverage separation techniques for active and maturing whitecaps, Methods in Oceanography, 8, 1-12, 10.1016/j.mio.2014.03.001, 2013.

Schwendeman, M., and Thomson, J.: Observations of whitecap coverage and the relation to wind stress, wave slope, and turbulent dissipation, Journal of Geophysical Research: Oceans, 120, 8346-8363, 10.1002/2015jc011196, 2015.

Stefels, J., Steinke, M., Turner, S., Malin, G., and Belviso, S.: Environmental constraints on the production and removal of the climatically active gas dimethylsulphide (DMS) and implications for ecosystem modelling, Biogeochem, 83, 245-275, 10.1007/s10533-007-9091-5, 2007.

Virkkula, A., Teinilä, K., Hillamo, R., Kerminen, V.-M., Saarikoski, S., Aurela, M., Koponen, I. K., and Kulmala, M.: Chemical size distributions of boundary layer aerosol over the Atlantic Ocean and at an Antarctic site, Journal of Geophysical Research-Atmospheres, 111, art. no.-D05306, 10.1029/2004jd004958, 2006.

Wanninkhof, R., Ledwell, J. R., and Broecker, W. S.: Gas exchange-wind speed relation measured with sulfur hexafluoride on a lake, Science, 227, 1224-1226, 10.1126/science.227.4691.1224, 1985.

Wanninkhof, R.: Relationship between wind speed and gas exchange over the ocean, J Geophys Res-Oceans, 97, 7373-7382, 1992.

Wanninkhof, R., and Knox, M.: Chemical enhancement of CO_2 exchange in natural waters, Limnology and Oceanography, 41, 689-697, 10.4319/lo.1996.41.4.0689, 1996.

Watson, A. J., Upstill-Goddard, R. C., and Liss, P. S.: Air-sea gas exchange in rough and stormy seas measured by a dual-tracer technique, Nature, 349, 145-147, 1991.

Weiss, R. F.: Carbon dioxide in water and seawater: The solubility of a non-ideal gas, Marine Chemistry, 2, 203-215, http://dx.doi.org/10.1016/0304-4203(74)90015-2, 1974.

Woolf, D. K.: Bubbles and the air-sea transfer velocity of gases, Atmosphere-Ocean, 31, 517-540, 1993.

Woolf, D. K.: Bubbles and their role in gas exchange, in: The Sea Surface and Global Change, edited by: Liss, P. S., and Duce, R. A., Cambridge University Press, Cambridge, 173-205, 1997.

Woolf, D. K.: Parametrization of gas transfer velocities and sea-state-dependent wave breaking, Tellus Series B-Chemical and Physical Meteorology, 57, 87-94, 2005.

Woolf, D. K., Leifer, I. S., Nightingale, P. D., Rhee, T. S., Bowyer, P., Caulliez, G., de Leeuw, G., Larsen, S. E., Liddicoat, M., Baker, J., and Andreae, M. O.: Modelling of bubble-mediated gas transfer: Fundamental principles and a laboratory test, Journal of Marine Systems, 66, 71-91, http://dx.doi.org/10.1016/j.jmarsys.2006.02.011, 2007.

Woolf, D. K., Land, P. E., Shutler, J. D., Goddijn-Murphy, L. M., and Donlon, C. J.: On the calculation of air-sea fluxes of CO_2 in the presence of temperature and salinity gradients, Journal of Geophysical Research: Oceans, 121, 1229-1248, 10.1002/2015jc011427, 2016.

Yang, M., Blomquist, B. W., Fairall, C. W., Archer, S. D., and Huebert, B. J.: Air-sea exchange of dimethylsulfide in the Southern Ocean: Measurements from SO GasEx compared to temperate and tropical regions, J Geophys Res-Oceans, 116, art. no.-C00F05, 10.1029/2010jc006526, 2011.

Yang, M., Beale, R., Liss, P., Johnson, M., Blomquist, B., and Nightingale, P.: Air-sea fluxes of oxygenated volatile organic compounds across the Atlantic Ocean, Atm Chem Phys, 14, 7499-7517, 10.5194/acp-14-7499-2014, 2014.

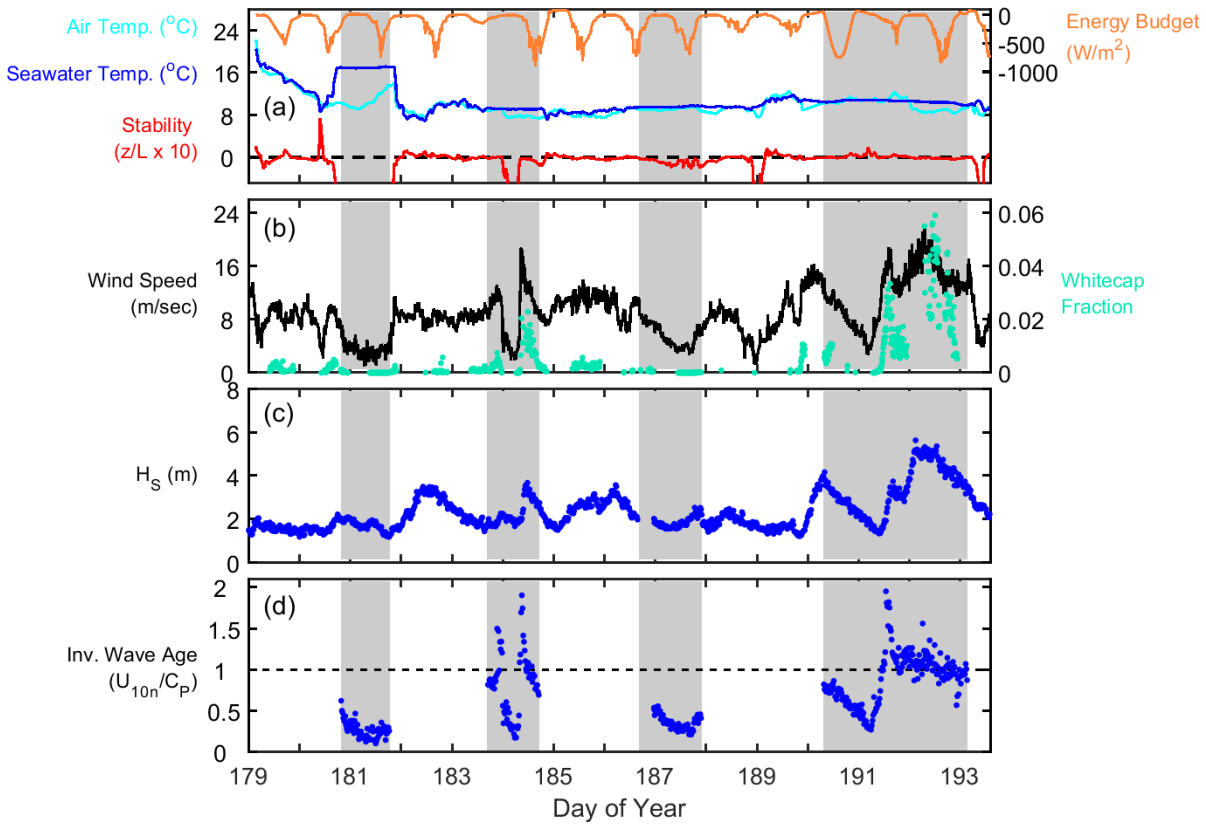

Figure 1: Time series of ten minute averaged data collected during the Knorr_11 cruise. Dashed black line in panel (a) indicates neutral atmospheric stability (z/L = 0). Grey shaded regions represent intervals when the ship occupied stations ST181, ST184, ST187, and ST191. Measured wave properties (see Bell et al., 2013) are presented in panel (c) and (d): ~~Panels (c), (d) and (e) are the~~significant wave height (H_s, c) and inverse wave age (d). $U_{10n}/C_p \geq 1$ represent younger seas and $U_{10n}/C_p < 1$ represent older seas. ~~CO_2 concentration difference (ΔpCO_2), flux (F_{CO2}) and gas transfer velocity (k_{CO2}) (water-side only, no *Sc* correction), respectively. Panel (e) also shows k_{CO2} calculated using the NOAA COARE model (black line). Note that negative k_{CO2} data points in (e) were omitted for clarity (see Supplemental Figure S2 for full data set).~~

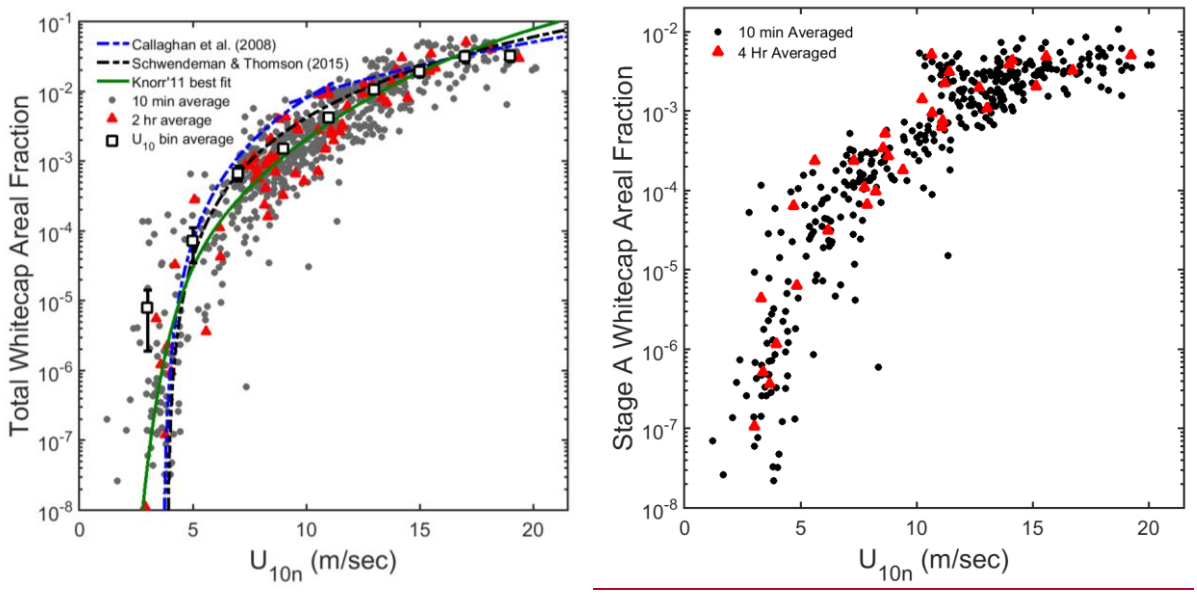

Figure 2: Semi-log plots of whitecap areal fraction as a function of mean horizontal wind speed at 10 m above the sea surface (U_{10n}) during the Knorr_11 cruise. 10 min average (grey dots) and 2 hour average (red triangles) data are shown on both panels. Left panel shows total whitecap area (W_T) versus U_{10n} bin averaged data (open squares, 2 m s^{-1} bins). The best fit line to Knorr'11 2 hr average data (green; $\log_{10}(W_T) = -42.19e^{(-0.95U)} - 6.5e^{(-0.0886U)}$) and wind speed parameterisations from the recent literature are shown for reference. Right panel is the whitecap area considered to be solely from wave breaking (Stage A whitecaps (W_A), see text for definition).

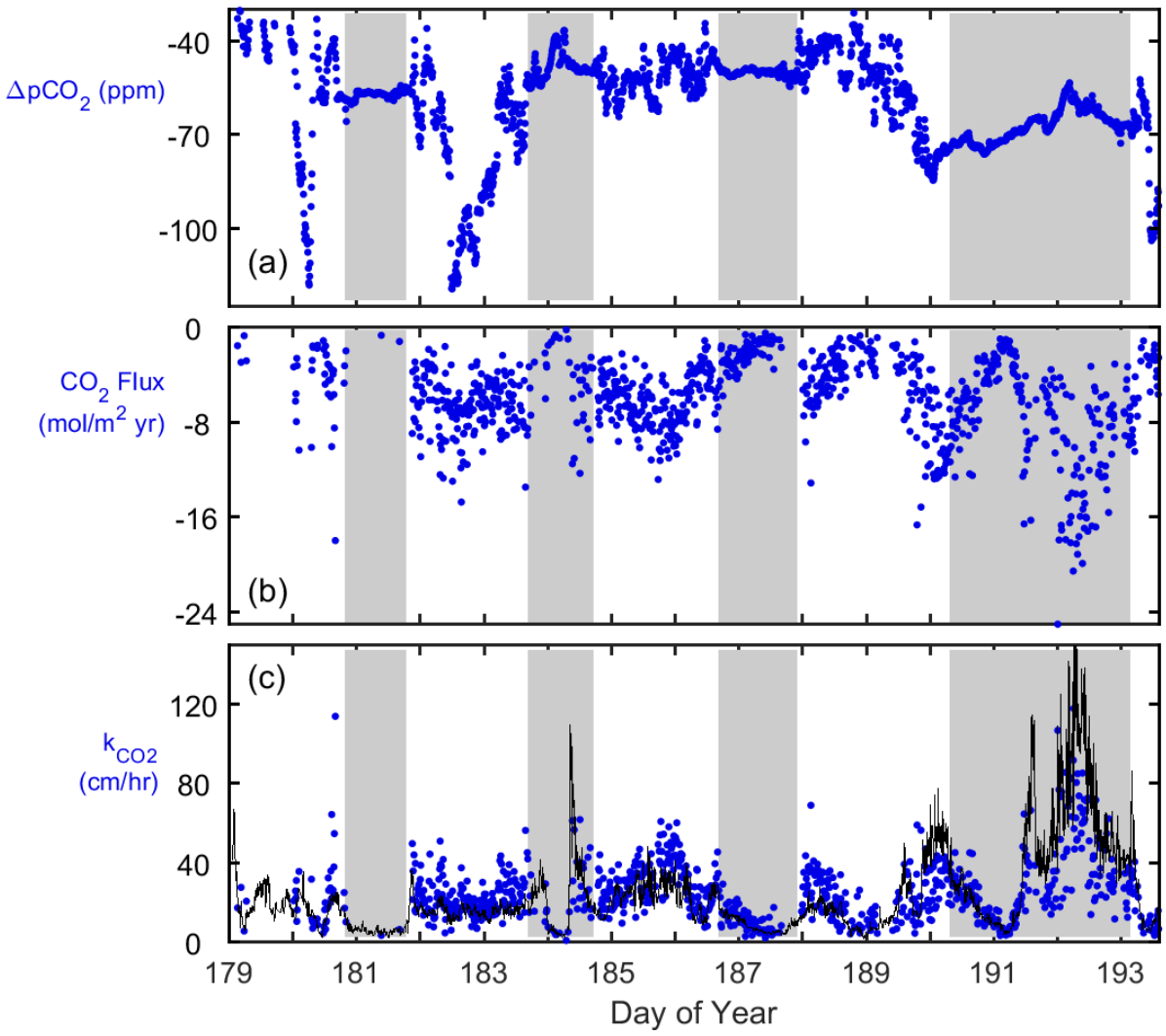

Figure 3: Knorr_11 cruise time series of ten minute averaged CO_2: (a) air/sea concentration difference (ΔpCO_2); (b) flux (F_{CO2}); and (c) gas transfer velocity (k_{CO2}) (water-side only, no *Sc* correction). Panel (c) also shows k_{CO2} calculated using the NOAA COARE model (black line). Note that negative k_{CO2} data points in (c) were omitted for clarity (see Supplemental Figure S6 for full data set). Grey shaded regions represent periods on station.

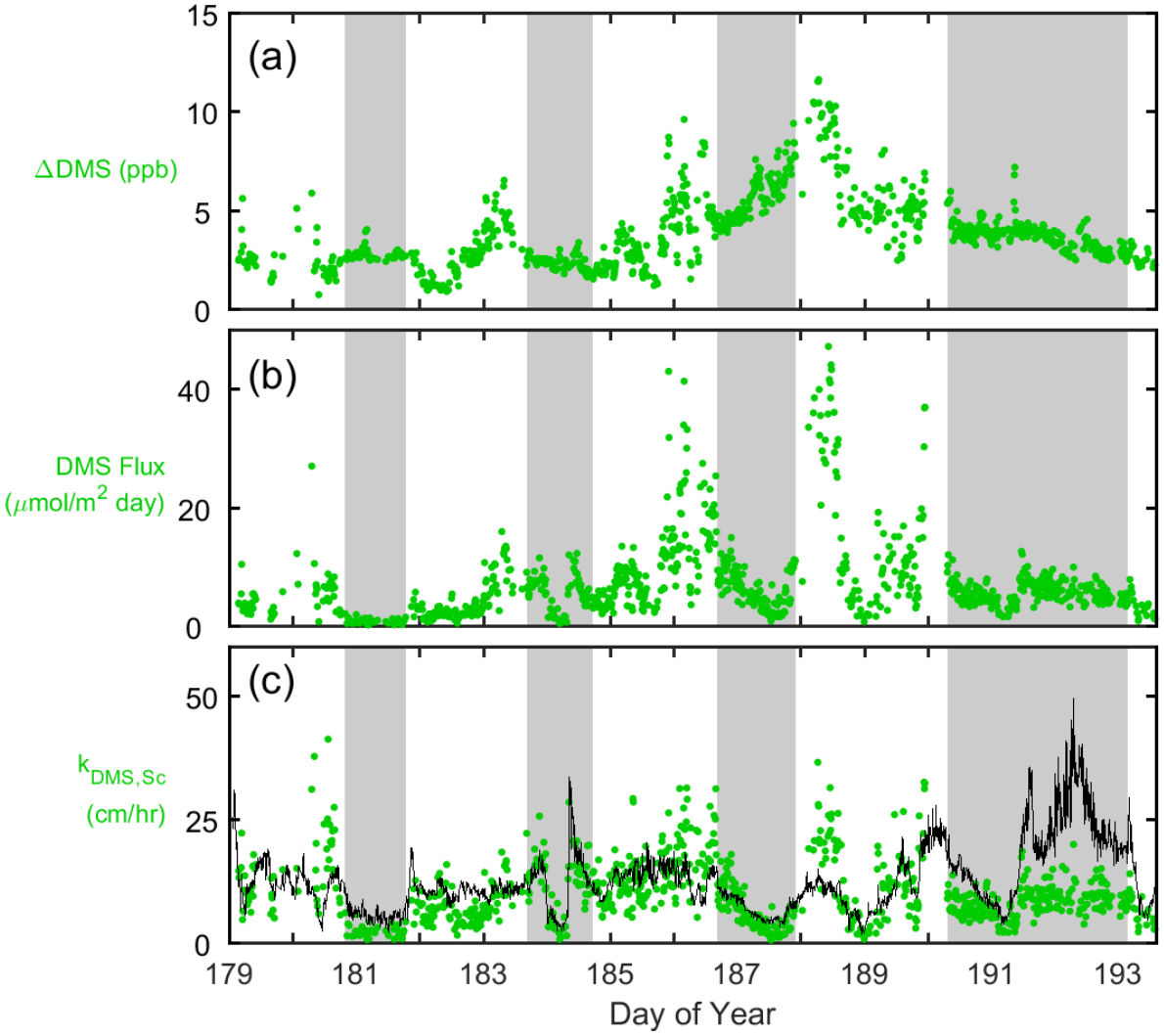

Figure ~~2~~4: Knorr_11 cruise time series of ten minute averaged DMS: (a) air/sea concentration difference (ΔDMS); (b) flux (F_{DMS}); and (c) gas transfer velocity normalised to the *in situ* CO_2 *Sc* number ($k_{DMS,Sc}$). Panel (c)~~,~~ shows $k_{DMS,Sc}$ calculated using NOAA COARE model output (black line). Grey shaded regions represent periods on station.

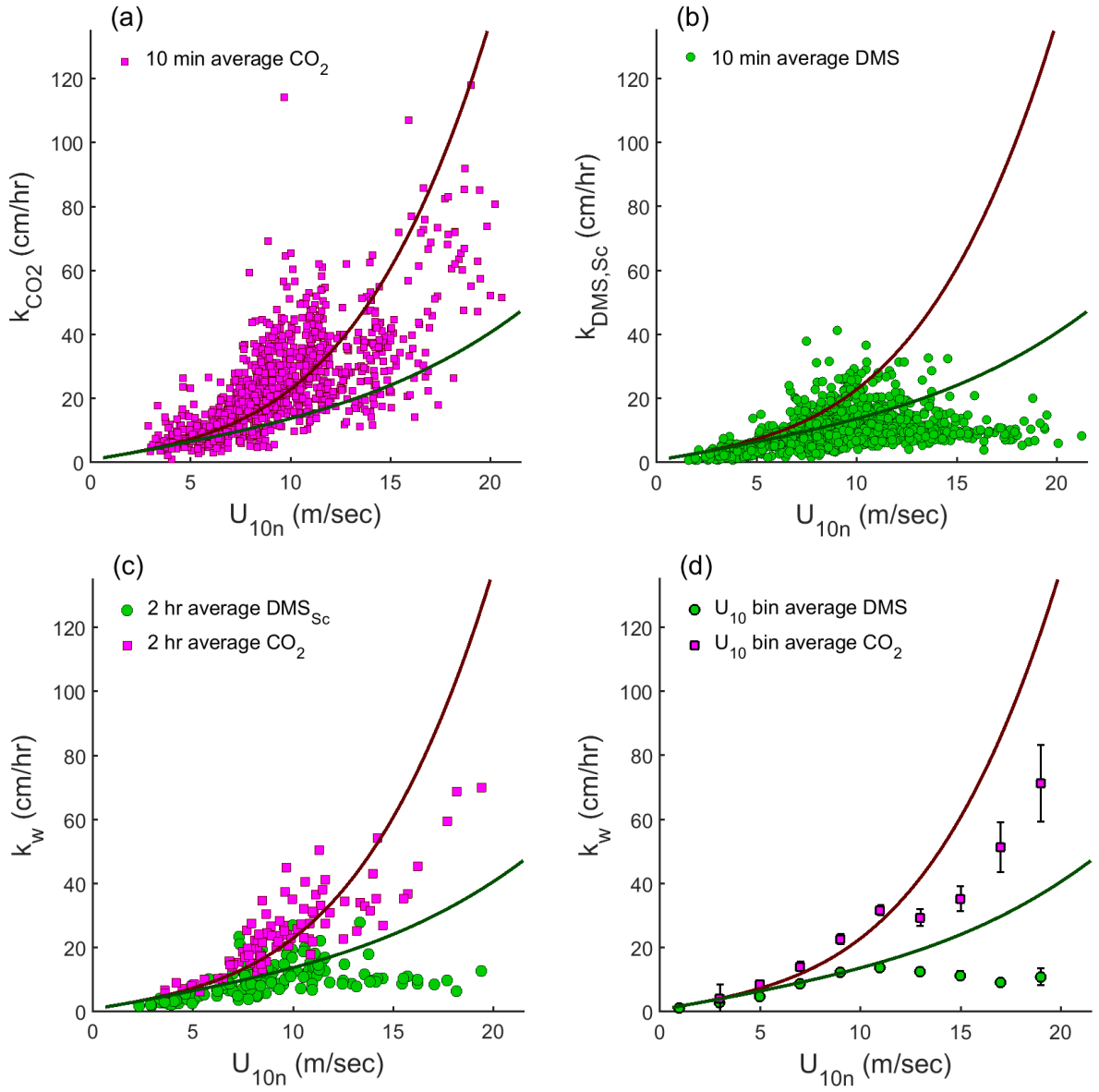

Figure 5: Gas transfer velocities plotted against mean horizontal wind speed (U_{10}) from the Knorr_11 cruise. Ten minute average data for CO_2 (a) and DMS (b). DMS gas transfer velocities are normalised to the *in situ* CO_2 *Sc* number. Data are averaged into 2~~4~~ hour periods (c) and 2 m s^{-1} wind speed bins (d). Note that negative k_{CO2} data in (a) ~~and (c)~~ have not been plotted for clarity (see Supplemental Figure ~~S4~~ S8 for full data set). For reference, the NOAA COAREG3.1 model output for CO_2 (magenta line) and DMS (green line) is plotted on all four panels. The COARE model was run with the turbulent/molecular coefficient, A = 1.6, and the bubble-mediated coefficient, B = 1.8, and used mean Knorr_11 data for the input parameters.

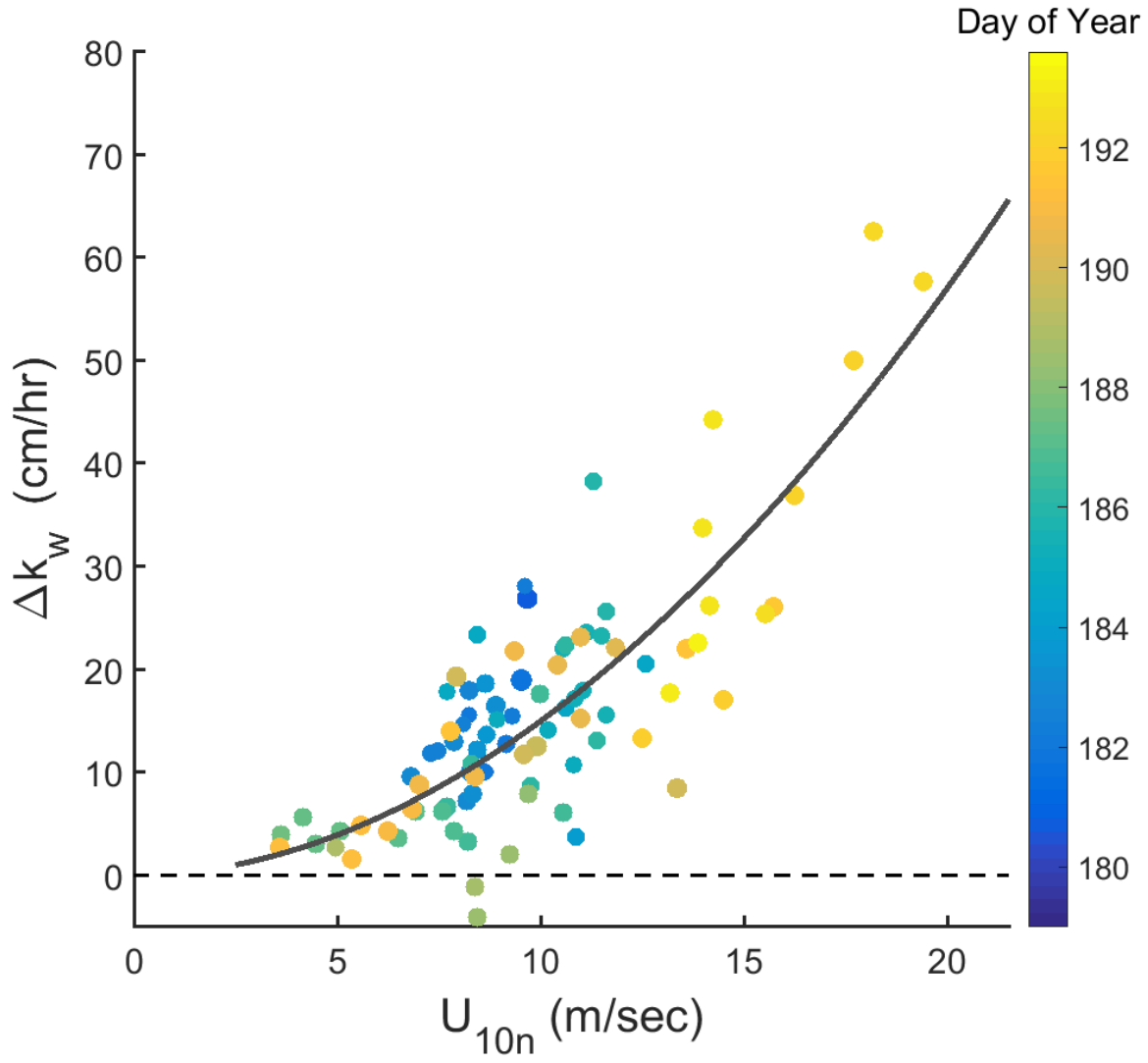

Figure 6: Difference (Δk_w) between 24 hour average k_{CO_2} and $k_{DMS,Sc}$ plotted against U_{10}. Data are coloured by the date of measurement (Day of Year). The solid grey line describes the power law fit to the data (see ~~text for coefficients~~ Equation 7).

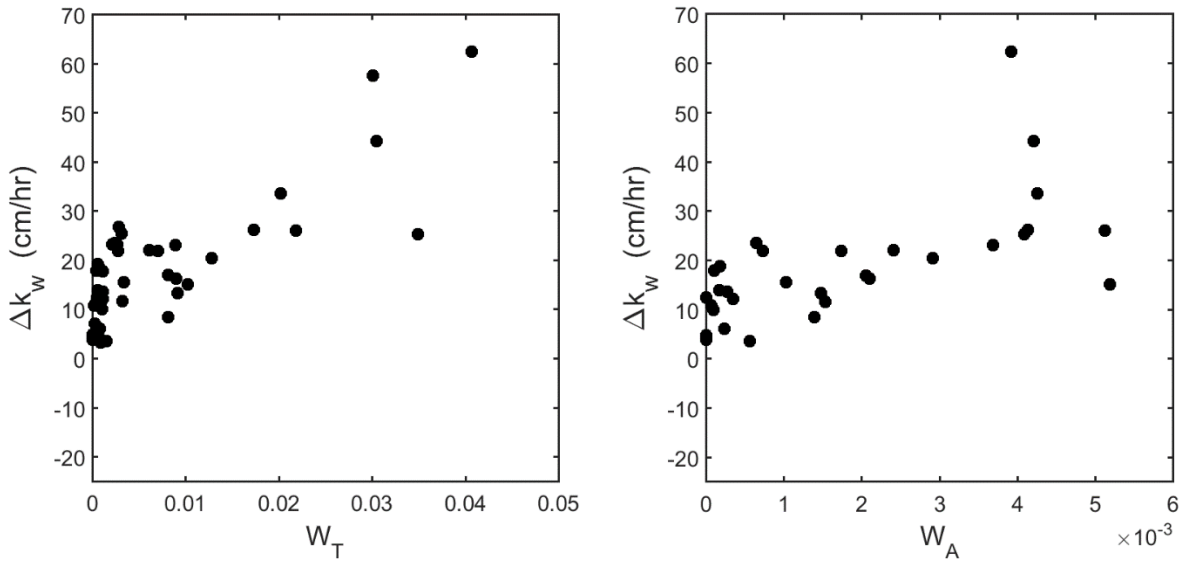

Figure 7: Knorr_11 Δk_w data plotted against total whitecap areal fraction (left panel) and against Stage A whitecap areal fraction (right panel). Each point is a 24 hour average of coincident measurements of whitecap fraction and DMS and CO_2 gas transfer.

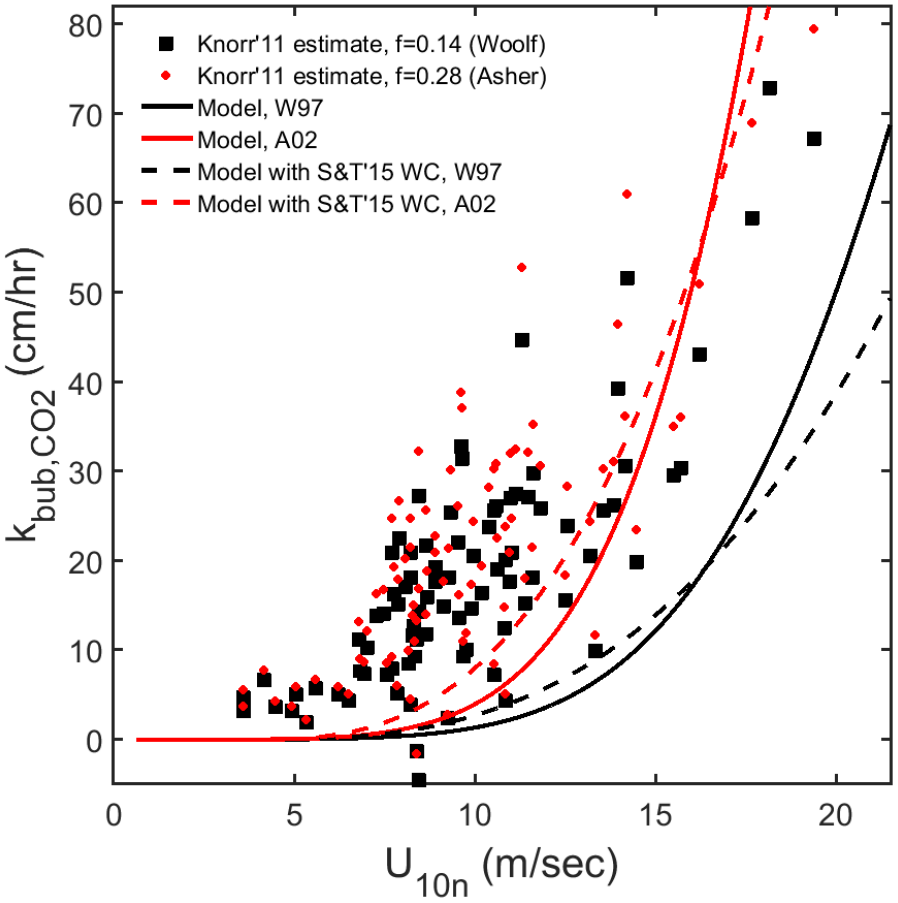

Figure 8: Bubble-mediated transfer velocity of CO_2 (k_{bub,CO_2}) as a function of wind speed. Individual points are Knorr_11 observations using solubility and diffusivity scaling from Woolf (1997) (black squares) and Asher et al. (2002) (red circles). Continuous lines are model calculations of k_{bub,CO_2} using the Knorr_11 wind speed-whitecap areal fraction relationship (see Figure 2) and mean SST (Woolf (1997), black; Asher et al. (2002), red). Model calculations were also performed using the Schwendeman and Thomson (2015) wind speed-whitecap areal fraction relationship (dashed lines).